# ABOLISHING MULTIDRUG RESISTANCE IN CULTURED LUNG CANCER CELLS WITH RNA INTERFERENCE.

**A THESIS [BIO 698 (6 CREDITS)]**

**SUBMITTED TO THE GRADUAL SCHOOL**

**IN PARTIAL FULFILLMENT OF THE REQUIREMENTS**

**FOR THE DEGREE OF**

**MASTERS OF SCIENCE**

**BY**

**KAMAL PRAJAPATI**

**ADVISOR**

**DR. CAROLYN VANN**

**BALL STATE UNIVERSITY**

**MUNCIE, INDIANA**

**JULY 2010**

## ABSTRACT


**TITLE:** Abolishing Multidrug Resistance in Cultured Lung Cancer Cells with RNA Interference

**STUDENT:** Kamal Prajapati

**DEGREE**: Masters of Science

**COLLEGE:** Science and Humanities

**DEPARTMENT:** Biology

**DATE:** July, 2010

**PAGES:**

The gene, *cox-1,* is over-expressed in cultured GLC4 small cell lung cancer cells concurrent with the development of multi-drug resistance (MDR) as a result of the use of the chemotherapeutic agent used to combat the cancer, doxorubicin. Prevention of MDR has been a tremendous challenge in cancer research and this research is concerned with abolishment of MDR as a cancer survival strategy. RNA-mediated interference technology (RNAi) was employed using siRNA to decrease *cox-1* expression and temporarily restore the susceptibility of the cells to doxorubicin. GLC4 cells are of three types: S (sensitive cells never exposed to doxorubicin); ADR (MDR cells cultured in doxorubicin), and; REV (revertant cells previously cultured in presence of doxorubicin but no longer). REV and ADR cells were transfected with *cox-1* siRNA. After 24 h, $1x10^6$ cells were used for RNA isolation and 1 µg of RNA was used for RT-PCR to assess

down-regulation of *cox-1* RNA. RT-PCR results indicated that *cox-1* RNA was down-regulated to basal levels seen before exposure to doxorubicin. Ct values for GLC4/ADR and *cox-1* down-regulated GLC4/ADR cells were 23 and 34, respectively. The result indicated abundant levels and moderate levels of *cox-1* mRNA in the ADR cells and the transfected ADR cells respectively. The relative expression level of *cox-1* mRNA was 33% higher in the non-transfected GLCR/ADR cells as compared to the transfected GLCR/ADR cells as shown by the curve. Two hundred thousand cells were used for hemacytometer cell counts in the presence of trypan blue to assess cell viability. *cox-1* down-regulation in ADR cells resulted in a significantly higher percentage of non-viable cells (25.4%) as compared to its non-transfected control (20.5%) using a Student's *t*-test (*P <0.05). Similarly, fluorescence microscopy confirmed that apoptosis was significantly increased in the ADR cells treated with doxorubicin and *cox-1* siRNA simultaneously (69.4%) as compared to its non-transfected control (56.7%) (*= P <0.01). A Western blot analysis performed by Fernando Cuadrado indicated that siRNA transfection decreased the expression of COX-1 by 66% in GLC4/ ADR cells as compared to the non-transfected control using densitometry. However, no conclusive results were obtained using flow cytometry as the flow cytometer was incapable of analyzing the mixed cell population (adherent and suspension) which is a characteristic of this cell line, GLC4. Thus, we have clearly demonstrated that MDR cancer cells can be altered temporarily to become susceptible to doxorubicin, a potentially important finding for the treatment of cancer patients.

## ACKNOWLEDGEMENTS

I would like to express my heartfelt gratitude to my thesis advisor, Dr. Carolyn Vann, for her intense support and guidance throughout this project. Her enthusiasm and motivation has always been the greatest factor in the successful completion of this project. I would also like to acknowledge my committee members Dr. James Olesen and Dr. John McKillip for their advice and also for letting me use their reagents and supplies.

I would like to thank Ian McIver for teaching me cell culture techniques, Sharmon Knecht for helping me with fluorescence microscopy, Dr. Heather Bruns for assistance with flow cytometry, Brandy Snider for her support, Dr. Hetty Timmer-Bosscha for providing me the cell lines, and Pratik Aryal for his technical advice. Similarly, there are other people whom I would like to thank for their teaching and support, especially Dr. Susan McDowell, Dr. Donald Ruch, Dr. Kemeul Badger, Susan Calvin, Janet Carmichael, Patricia Kleeber, Jay Anderson, and Bikram Sharma.

My special thanks also go to all the people in our research group for lending me their hands when the experiments were going on. Our research group consisted of Sloan Burdick, Staci Weaver, Matthew Green, Emmanuel Kwame, and Fernando Cuadrado. I would especially like to thank Fernando for performing Western analysis.

My sincere regards also go to my father Ganesh Man Prajapati, my mother Gyanu Maya Prajapati, and my entire family for providing me support and opportunities to ensure I received a high quality education for my future career.

Finally, I also would like to thank Indiana Academy of Sciences for funding this project.

**TABLE OF CONTENTS**

## LIST OF TABLES

## LIST OF FIGURES

## LIST OF ABBREVIATIONS

| | |
|---|---|
| **µg:** | **microgram** |
| **µl:** | **microliter** |
| **cDNA:** | **complementary DNA** |
| **COX:** | **cyclooxygenase** |
| **DNA:** | **deoxyribonucleic acid** |
| **ds:** | **double stranded** |
| **FBS:** | **fetal bovine serum** |
| **GLC4:** | **small cell lung cancer cell line** |
| **GLC4/S:** | **small cell lung cancer cell line sensitive to adriamycin (doxorubicin)** |
| **GLC4/ADR:** | **small cell lung cancer cell line resistant to adriamycin** |
| **GLC4/REV:** | **small cell lung cancer cell line resistant to adriamycin but not cultured in it** |
| **h:** | **hour** |
| **kDa:** | **kilodalton** |
| **MDR:** | **multidrug resistance** |
| **ml:** | **milliliter** |
| **nm:** | **nanometer** |
| **nM:** | **nanomolar** |
| **PTGS:** | **prostaglandin H synthase** |
| **RNA:** | **ribonucleic acid** |
| **RNAi:** | **ribonucleic acid interference** |
| **RT-PCR:** | **reverse transcriptase polymerase chain reaction** |
| **S:** | **sensitive** |
| **siRNA:** | **silencing RNA** |
| **U:** | **units** |

# INTRODUCTION

Lung cancer is the most prevalent type of cancer among both sexes in United States (an estimated 213,380 new cases of lung cancer were diagnosed in 2007, representing about 15% of all cancer diagnoses) (American Cancer Society, 2007). The two different types of lung cancer which are characterized according to the cell size of the tumor are small cell lung cancer (SCLC) and non small cell lung cancer (NSCLC). SCLC cells are small with a prominent nucleus, unlike NSCLC cells. Both these types of cancer are mainly caused by smoking and exposure to asbestos (U.S. Department of Health and Human Services, 2008). Lung cancer has a very low five-year survival rate (15.6%) as compared to other cancers (American Lung Association, 2009; U.S. National Institutes of Health, 2009). It is a very aggressive tumor type with a great tendency to metastasize (Jemal et al., 2008; Schreiber et al., 2008; Emedicine, 2009). In 2006 $9.6 billion of the $206 billion provided to combat cancer treatment in the United States was spent on lung cancer treatment, indicating that lung cancer is one of the most expensive cancers to treat (Centers for Disease Control and Prevention, 2007; U.S. National Institutes of Health, 2009).

Because the majority of the SCLC diagnosed patients have metastasis, localized forms of treatment such as surgery and radiation therapy are generally ineffective.

Chemotherapy, the most effective mode of treatment, becomes ineffective after development of multi-drug resistance (MDR). With the development of MDR, chemotherapeutic drugs such as doxorubicin become ineffective as expression of ATP-binding cassette transporters efflux the drugs to the outside of the cell thus decreasing cellular drug accumulation (Ambudkar et al., 1999; Gottesman et. al., 2002). Then the cancer cells no longer die by apoptosis.

We postulated that restoration of apoptosis in cultured SCLC MDR cancer cells might permit the chemotherapeutic drug doxorubicin to kill the previously resistant cancer cells. Previously, we found increased levels of both *cox-1* mRNA and COX-1 protein and decreased apoptosis in MDR cells (Aryal, 2007). Thus, we used RNA interference technology (RNAi) to down-regulate *cox-1* expression temporarily by the introduction of a specific *cox-1* siRNA (silencing RNA) into cultured cells in the presence and absence of doxorubicin. The experiment was performed in triplicate and results were assessed using flow cytometry, fluorescence microscopy, RT-PCR and Western analysis to determine whether MDR was reversed.

The results of this research are expected to provide a better understanding of the MDR mechanism in GLC4 cells. It is known that extended cellular inflammation can lead to cancer (Wu et al., 1995). We also know that with MDR development we observe a loss of apoptosis and, in the GLC4 cells, an increase in expression of COX-1 protein (Aryal, 2007). Since COX-1 is a pro-inflammatory protein, this suggests that inflammation also plays a role in the development of MDR. Thus, we want to determine if down- regulation of *cox-1* in GLC4/ADR cells will restore apoptosis and help to prevent MDR. If RNAi inhibition of the expression of *cox-1* in transfected cells inhibits

the normal growth of the MDR cancer cells and makes them more temporarily sensitive to chemotherapy, this finding would have important medical implications for cancer patients. Even a temporary reduction in expression of *cox-1* by siRNA introduction might provide enough time for chemotherapeutic drugs to be administered and the protocol could be repeated if needed. Thus, the results of this research could have significant implications for the treatment of MDR cancer by down-regulating the inflammatory gene, *cox-1*.

# REVIEW OF THE LITERATURE

## Lung Cancer and Small Cell Lung Cancer (SCLC):

Transformation of a normal lung cell can lead to two different types of cancer characterized according to the cell size of the tumor as either small cell lung cancer (SCLC) or non small cell lung cancer (NSCLC**)**. SCLC cells are small with a prominent nucleus. Contrary to this, NSCLC cells are not small and are further divided as adenocarcinoma, squamous cell carcinoma, and large cell carcinoma. Both these types of cancer are mainly caused from smoking or exposure to asbestos (U.S. Department of Health and Human Services, 2008).

The lung cancer five-year survival rate is very low (3.5%) once the cancer has spread to other organs, so that most lung cancer patients die within one year of being diagnosed (Emedicine, 2009). The median survival rate without treatment of SCLC is only 2 to 4 months. Collins et al. (2007) classified SCLC as *limited stage* if it was present within the scope of a single radiotherapy field and was limited to one half of the chest. If the cancer exceeded these limits, it was referred to as *extensive stage*. Even with treatments available today, SCLC in its extensive form has shown only a limited increase in the 2-year survival rate from 1.5% in 1973 to only 4.6% in 2000 (Govindan et al., 2006; American Cancer Society, 2007).

A frequent metastasis site following primary lung cancer is the brain. Fig. 1 shows a secondary cancer site resulting from metastasis using a contrast-enhanced MRI of the brain from a SCLC patient (Emedicine, 2008). In the figure, the two rings mark the metastatic lesions in the periventricular region in the axial section at the level of lateral ventricles.

**Multi-Drug Resistance (MDR):**

Chemotherapy is the most effective means to treat SCLC but a common failure in chemotherapeutic treatment is the development of multi-drug resistance (MDR). With the development of MDR, chemotherapeutic drugs become ineffective as expression of ATP-binding cassette transporters efflux the drugs to the outside of the cell thus decreasing cellular drug accumulation (Ambudkar et al., 1999; Gottesman et. al., 2002). This results no apoptosis in the cancer cells which would normally be detected as abnormal by the immune system and induced to die. The most frequently used cytotoxic drugs used in chemotherapy are hydrophobic, amphipathic natural products, such as taxanes, vinca alkaloids, anthracyclines (doxorubicin, daunorubicin, epirubicin), epipodophyllotoxins, topotecan, dactinomycin, and mitomycin C (Ambudkar et al., 1999; Krishna et al., 2000).

Since doxorubicin was used as a chemotherapeutic drug in earlier studies in this particular cell line, this experiment also uses it to achieve MDR condition in GLC4/ADR cells. Doxorubicin is believed to interact with DNA by intercalation to inhibit macromolecular biosynthesis (Momparler et al., 1976; Fornari et al., 1994). Specifically, doxorubicin inhibits progression of the enzyme topoisomerase II which unwinds DNA for transcription. Doxorubicin binding stabilizes the topoisomerase II complex after it

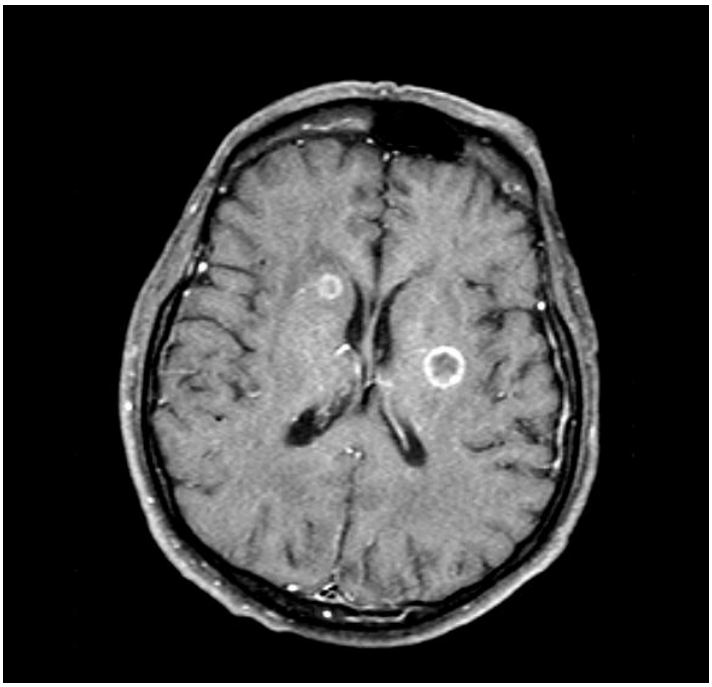

**Fig. 1: Contrast-enhanced MRI of the brain of a SCLC patient**. Two ring-enhancing metastatic lesions in the periventricular region are shown in the axial section at the level of lateral ventricles (Emedicine, 2008).

has broken the DNA chain for replication. This prevents the DNA double helix from being resealed and stops the process of replication.

After exposure of cancer cells to a chemotherapeutic agent such as doxorubicin for a length of time, MDR often develops. Then, the cell is genetically altered (including an up-regulation in membrane pumps to efflux the drug) and the cell is not only resistant to the administered drug, but also to a wide variety of other drugs. Mechanisms contributing to MDR development have been classified as non-cellular and cellular types. When extracellular factors such as limited vascular accessibility or cell growth environment are shown to have a key role then it is considered to be of non-cellular type. Similarly, the mechanism type is classified as cellular when referring to enzymes and transport systems (Fan et al., 1994). The non-cellular mechanisms are normally observed in those cancer types which show natural resistance to chemotherapy at the time of the addition of the drug. For example, poor vasculature is associated with certain solid tumors such that the drugs cannot reach the cancer cells and this limits the cytotoxicity of the drug (Jain, 1987). Poor vasculature around the tumor cells results in a lack of nutrition, hypoxia, and the accumulation of lactic acid. Thus, drug resistance or MDR development may depend on the presence of actively dividing, well-nourished cancer cells (Demant et al., 1990).

Cellular MDR mechanisms may be classified as non-classical/non-transport based or classical/transport based mechanisms. Enzyme systems that limit the desired activity of the drug without altering its effective concentration inside the cell are included under the non-transport based cellular MDR mechanisms. Among such enzymes, glutathione-S-transferase (GST) is an important one in xenobiotic metabolism which catalyzes the

biotransformation of organic molecules by conjugating them with polar molecules to facilitate their excretion. According to previous studies, GST mediates biotransformation of various anticancer drugs and its increased level was observed in resistant breast cancer cell lines such as MCF-7 (Batist et al., 1986; Hao et al., 1994). The chemotherapeutic drugs are modified into an end product with reduced activity and an enhanced rate of excretion with over-expression of GST.

In contrast, under the transport based classical cellular mechanism, the drugs are effluxed from the cell by various energy-dependent membrane transport proteins which prevent them from reaching therapeutic concentrations inside the cell (Gottesman, 2002). The family of proteins responsible for the efflux includes the ATP-binding cassette (ABC) transporters which are ATP-dependent. The ABC super family consists of transport proteins such as P-glycoprotein (P-pg), also known as multi-drug resistance-associated protein-1 (MRP1), its homolog MRP2-6, and the breast cancer resistance protein (BCRP) (Riordan et al., 1985; Doyle et al., 1998; Borst et al., 2000). All of these have been found to be over-expressed in malignant cells, where they serve to pump anticancer drugs out of the cell resulting in a reduction of intracellular drug levels necessary for effective therapy (Leonard et al., 2003; Choi, 2005).

P-glycoprotein or MDR1 was the first multi-drug transporter to be discovered and it is also the most studied and well-characterized transporter (Chen et al., 1986; Ambudkar et al., 1992; Gottesman and Pastan, 1993). The transmembrane regions of P-gp form the drug translocation pathway (Loo and Clarke, 2001), while the ATP-binding sites with ATPase activity provide the metabolic energy enabling the drug efflux (Higgins, 1992). Nakamura et al. (2000) showed that P-gp is normally expressed in the

transport epithelium of the kidney, liver and gastrointestinal tract, tissues which usually have the highest expression of P-gp when tumors develop and which are most likely to develop MDR. A partial recovery of intracellular drug accumulation was followed by the down-regulation of P-gp (Xu et al., 2006).

A few compounds have been studied which have the ability to reverse MDR and they are called MDR inhibitors, chemosensitizers, or MDR modulators (Kellen, 2003). A promising study done on natural MDR modulators by Limtrakul et al. (2007) reported MDR reversal against vinblastine, paclitaxel and colchicines in KB-V1 cells (MDR human cervical carcinoma with high P-gp expression) after a dose dependent use of root extract from *Stemona curtisii*. Previous studies carried out by Schoenlein (1994) showed that drug-resistant KB-V1 cells expressed P-gp at high levels on their plasma membranes and that *S. curtisii* root extract modulated P-gp activity and reversal of the MDR phenotype. Also, Fong et al. (2007) showed that rhizome extracts of *Alisma orientalis* have a synergistic growth inhibitory effect when used with cancer drugs targeting over-expressed P-gp including doxorubicin, actinomycin D, vinblastine, puromycin in MDR HepG2-DR and K562-DR cells. In addition, they showed the combination was more effective than verapamil (a standard P-gp inhibitor) alone in enhancing cellular doxorubicin accumulation. Similarly, flavonoids, a major class of natural compounds widely present in foods and herbal products, have been found to inhibit the breast cancer resistance protein (BCRP) which has a significant role in drug cellular disposition (Shuzhong et al., 2005). Honokiol is another natural compound present in a Chinese medicinal herb *(Magnolia grandiflora*) which can fight cancer by inhibiting angiogenesis, inducing apoptosis and, down-regulating the expression of P-glycoprotein

in MCF-7/ADR (human breast MDR cancer) at both the mRNA and protein levels. However, only doxorubicin has been considered in this study since most of the previous studies on this SCLC cell line has been conducted using doxorubicin.

Thus, when MDR develops, anticancer drugs are no longer effective in inhibiting cancer cell proliferation for a number of reasons including variations in the absorption, metabolism and delivery of drug to target tissues and if the tumor is located in parts of the body where the drugs cannot easily penetrate. Understanding the molecular mechanism of MDR has become a major challenge for cancer researchers. If we can fully understand factors influencing its development then we may be able to reverse MDR in cancer cells, thus making MDR cells sensitive again to anti-cancer drugs.

**Apoptosis and Necrosis:**

Apoptosis is gene-regulated programmed cell death (PCD) where cells undergo death to control excessive proliferation or in response to some genetic or cellular damage. The term was first coined by Kerr, Wyllie and Currie in 1972. PCD involves a series of biochemical events leading to morphological changes such as blebbing of cells, loss of membrane asymmetry, cell shrinkage, and nuclear, chromatin and chromosomal DNA fragmentation (Kerr et al., 1972; Lowe et al., 2000). Resistance to normal apoptosis is a key factor for survival and growth of cancer cells. In addition, defects in apoptosis signaling can contribute to MDR. Thus, a primary goal for cancer treatment is to restore normal apoptosis in cancer cells.

Various cell signals originating either extracellularly or intracellularly control the process of apoptosis. Some of the extracellular signals frequently discussed include toxins, hormones, growth factors, nitric oxide or cytokines (Popov et al., 2002; Brune et

al., 2003). A response occurs once they cross the plasma membrane. These signals may positively or negatively affect apoptosis.

Intracellular apoptotic signaling in a cell is initiated in response to a stress which may result in cell suicide. Release of intracellular apoptotic signals by a damaged cell is triggered by various factors such as heat, radiation, viral infection, nutrient deprivation, binding of nuclear receptors by glucocorticoids, hypoxia, and elevated intracellular calcium concentration (Elmore et al., 2007; Henshall et al., 2007). Apoptosis is also thought to be regulated by cellular components such as Poly ADP ribose polymerase which is a protein involved in a number of cellular processes involving mainly programmed cell death and DNA repair.

The apoptosis pathway is initiated by regulatory proteins after it is instructed by the apoptotic signals to do so. Apoptotic signals either cause cell death or the process can be stopped such that the cells no longer need to die. Targeting mitochondria functionality, or directly transducing the signal via adaptor proteins to the apoptotic mechanisms are two main methods of regulation that have been identified. Mitochondria could possibly be contributing to apoptosis signaling via the production of reactive oxygen species (Wang et al., 2001). Similarly, the adaptor proteins such as MyD88 tend to lack any intrinsic enzymatic activity themselves but instead mediate specific protein-protein interactions which drive the formation of protein complexes (Aliprantis et al., 1999). Increase in calcium concentration within a cell due to drug activity is another extrinsic pathway for initiation which is identified in several toxin studies. In this case, apoptosis results via a calcium binding protease called calpain (Henshall et al., 2007).

Nitric oxide can induce apoptosis by helping to dissipate the membrane

potential of mitochondria and making it more permeable (Fink et al., 2005). With an increase in permeability, mitochondrial proteins such as SMACs (second mitochondria-derived activator of caspases) are released into the cytosol. SMAC then binds to inhibitor of apoptosis proteins (IAPs) to deactivate them. This prevents the IAPs from arresting the apoptotic process, permitting apoptosis to proceed. Normally IAPs also suppress activity of a group of cysteine proteases called caspases, which are responsible for the cell degradation. Thus, in this process, mitochondrial permeability is indirectly regulating the actual degradation of enzymes.

In mammals, direct initiation of apoptotic mechanisms are most likely observed via the TNF-induced (tumor necrosis factor) model and the Fas-Fas ligand-mediated model. These models involve receptors of the TNF receptor (TNFR) family coupled to extrinsic signals (Wajant et al., 2002). Activated macrophages are responsible for the production of cytokine TNF which is part of the extrinsic pathway for triggering apoptosis. Previous studies have found that close association of TNF-R with that of procaspases has been found through adapter proteins (FADD, TRADD) such that other inactive procaspases are cleaved (Chen et al., 2002). This triggers the caspase cascade, irreversibly resulting in apoptosis of the cell.

The Fas receptor binds the Fas ligand (FasL) which is a transmembrane protein part of the TNF family. Death-inducing signaling complex (DISC), which contains FADD, activates caspase-8 and caspase-10 due to the interaction between Fas and FasL (Murphy et al., 2000; Reich et al., 2008). TNF- R1 and Fas activation in mammalian cells is followed by a balance between pro-apoptotic and anti-apoptotic members of the *Bcl-2* family where the pro-apoptotic homodimers are responsible for the

release of caspase activators such as cytochrome c and SMAC by making the mitochondrial membrane permeable. Thus, most of the apoptotic pathway exists in a caspase-dependent mechanism. However, AIF (apoptosis-inducing factor) mediates a caspase-independent apoptotic pathway by causing DNA fragmentation and chromatin condensation (Susin et al., 1999).

Unlike apoptosis, necrosis is not a natural type of death as cells do not undergo the same chemical reactions as compared to apoptotic tissue. Necrosis is a non-physiological premature cell death due to external sources such as injury, infection, infarction, cancer, and inflammation (Fink et al., 2005). Necrosis usually starts with swelling of cells, digestion of chromatin and disruption of the organelle membranes and plasma membrane. Characterization of late necrosis is confirmed by extensive DNA hydrolysis, vacuolation of the endoplasmic reticulum, breakdown of organelle, and cell lysis. The main cause of inflammation in necrosis is due to the release of intracellular content after the rupture of the plasma membrane (Vakkila et al., 2004). Cells undergoing necrosis release harmful chemicals which are enzymes that are stored by lysosomes into the surrounding tissue. Enzymes contained in such lysosomes are released after they get damaged resulting the destruction of other parts of the cell. A chain reaction of further cell death is triggered if these enzymes are released from the non-dead cell.

RNA interference (RNAi) technology will be used in this project to down-regulate *cox-1* such that an increased percentage of apoptosis will be observed. Hemacytometer cell count using trypan blue dye will only assess the percentage of viability where trypan blue is picked up by non-viable cells with defective membranes.

So, apoptosis assay will be performed using flow cytometry and fluorescence microscopy. Apoptosis/necrosis detection kit (Enzo Life Sciences, Plymouth Meeting, PA) used during fluorescence microscopy actually differentiates apoptosis from necrosis. An Annexin V-EnzoGold (enhanced Cyanine-3) conjugate enables detection of apoptosis while the Necrosis Detection Reagent similar to the red-emitting dye 7-AAD, facilitates late apoptosis and necrosis detection.

**RNA Interference Technology:**

Nobel laureates, Andrew Fire and Craig Mello, in 1998 discovered that injection of small segments of double-stranded (ds) RNA in *C. elegans* would lead to effective degradation of specific, homologous cytoplasmic mRNAs. It is thought that this process is based on an evolutionarily conserved mechanism designed to protect against the expression of foreign RNA that might enter a cell. The down-regulation of expression occurs through a multi-step process in which longer viral RNA is reduced to small interfering RNA by the action of an RNase III endonuclease, Dicer. Then, numerous secondary molecules of interfering RNA (RNAi) are produced to bind any homologous RNA, causing its degradation. Down-regulation can also be triggered by the direct introduction of short double-stranded RNA (dsRNA) of approximately 21-27 nucleotides as Fire and Mello observed. The dsRNA may be introduced in a "naked" form called siRNA (small interfering RNA) for short-term effects or expression may be extended by cloning the dsRNA into a vector before introduction, called shRNA (small hairpin RNA). siRNA facilitates the cleavage and degradation of its recognized mRNA once it gets incorporated into the RNA-induced silencing complex (RISC) (Zhang et al., 2007). The

advantage of this would be specific down-regulation of our target mRNA which is often employed in experimental biology to study the function of genes in cell culture and *in vivo* in model organisms.

However, in some cases, long-term changes in gene expression by the introduction of shRNA can be detrimental (Grimm et al., 2007). Permanent knock down of a gene may not be beneficial as some of these genes may still be important for other regular functions. For instance, *cox-1* is a pro-inflammatory gene and if it is permanently knocked down then wound and infection would never be healed. shRNA contains a sense strand, antisense strand, and a short loop sequence between these two fragments. Such RNA molecules tend to form hairpin-shaped dsRNA as the sense and antisense fragments are complementary in their sequence. shRNA is cloned into a vector and a polymerase III type promoter is used for its expression. The expressed shRNA is finally exported into the cytoplasm where Dicer processes it into siRNA. This is followed by the incorporation of siRNA into the RISC.

According to George et al. (2001), COX-1 protein was one of several up-regulated proteins in SCLC cells exhibiting MDR. Because we believe this up-regulation may be central to the development of MDR, we used siRNA technology in this research to down-regulate the expression of *cox-1* mRNA to reduce the production of COX-1 protein. Use of siRNA would be a novel approach as previous studies have tried using COX-1 inhibitor such as SC-560 for the down-regulation (Lampiasi et al., 2006). Also, using siRNA has no detrimental effect unlike shRNA.

**Inflammation and COX Enzymes**

Inflammation is a response to acute tissue damage which results from some type of physical injury, infection or exposure to toxins (Balkwill et al., 2001; Coussens et al., 2002; Kuper et al., 2002). It is known that it aids in suppression of tumors by stimulation of an antitumor immune response. However, it also appears to stimulate tumor development. Chronic inflammation often has been associated with an increased risk of certain cancers according to epidemiologic and clinical research. Inflammatory bowel diseases such as ulcerative colitis and Crohn's disease, ultimately leading to cancers of the intestinal tract, are clear examples of this.

Infection is a common cause of inflammation (Munger et al., 2002). Previous evidence indicates that the presence of microbes can be a cofactor in the tumor promoting effects of inflammation. However, a clear pathway or mechanism is still unknown. Clinical trials of anti-inflammatory drugs (e.g., COX-2 inhibitors designed to inhibit this enzyme associated with inflammatory response) for cancer prophylaxis and treatment show inflammation as a potential area of cancer prevention (National Cancer Institute, 2009).

Cyclooxygenase (COX) is a term widely known for enzymes responsible for the formation of prostanoids. Prostaglandins, prostacyclin, and thromboxane are the three main groups of prostanoids which function in the inflammatory response. The initial step in the metabolism of arachidonic acid to intermediate prostaglandins is catalyzed by COX enzymes with both oxygenase and peroxidase activities (Smith et al., 1996). It is followed by conversions to other prostaglandins and thromboxanes by cell specific enzymes (Dupouy et al., 2006). COX-1, COX-2, and COX-3 are three isoenzymes but COX-3 is considered to be a variant of COX-1. Although COX-1 and COX-2 have the

same catalytic domains, only 65% amino acid similarity is shared by them. COX-1 is a constitutively expressed enzyme localized primarily in the endoplasmic reticulum (Morita et al., 1995) which functions to maintain the normal lining of the stomach in the gastrointestinal tract (Hawkey et al., 2001). In some carcinomas, its expression is found to be up-regulated. COX-2 is an inducible enzyme primarily present at sites of inflammation which is less frequently associated with development of cancer.

COX-1 which plays a key role in the metabolism of arachidonic acid and cancer cell growth is stimulated by increased levels of arachidonic acid. According to Gavett et al. (1999), COX-1 was an important component in the biosynthesis of prostaglandin in the mouse lung. An increased level of prostaglandin in the lung is one symptom of lung cancer (Vane et al., 1998). The level of expression of COX-1 has found to be elevated in other cancers such as colorectal, ovarian, and breast cancers (Hwang et al., 1998). Endothelial cell-derived COX-1 may also play a significant role in the angiogenic response of colorectal cancer (Tsujii et al., 1998*)*. Nonsteroidal Anti-inflammatory Drugs (NSAIDs) can provide relief from inflammation and pain by pharmacological inhibition of excessive COX production (Smith et al., 1971; Vane J.R, 1971).

Angiogenesis was found to be regulated by high levels of COX-1 expression in endothelial cells (Tsujii et al., 1998) where induced over-expression led to malignant transformation (Narko et al., 1997). Studies of colon polyp formation in Min mice (Chulada et al., 2000) found the disruption of either the *cox-1* or *cox-2* genes reduced the incidence of polyp formation, suggesting that key roles in cancer development may be played by both *cox* gene products.

SC-560 (a COX-1 inhibitor) is a member of the diaryl heterocycle class of cyclooxygenase inhibitors. The inhibitory effects of SC-560 result from inhibited cell proliferation as well as accelerated apoptosis as was observed in an ovarian cancer model (Li et al., 2008). It was determined that SC-560, in combination with ibuprofen, a non-selective NSAID, proved to be most effective at promoting tumor responsiveness to all agents involved. Furthermore, SC-560 was shown to indirectly limit tumor angiogenesis in ovarian cancer cells. Similarly, for the prevention of lung cancer in multiple phases IIb tests, inhibitors of the enzymes, zileuton (5-LOX), celecoxib (COX-2), and sulindac (COX-1 and COX-2) have been studied (Pepin et al., 1992).

*cox-1* was one mRNA found to be up-regulated in breast cancer cells as a result of doxorubicin selection by George et al. (2001). The increased production of *cox-1* and its central role in prostaglandin production is shown in Fig. 2 derived from that paper. Doxorubicin stimulates ceramide formation which is followed by caspase activation, and ultimately apoptosis in many cell types. In this figure, genes included in boxes had increased expression while those present in ovals had reduced expression after doxorubicin selection. In MDR cells, alterations in gene expression could be taking place in order to decrease in the apoptotic process and increase the resistance to doxorubicin toxicity. In another article, *cox-1* inhibition resulted in growth inhibition of epithelial ovarian tumors in mice, also indicating that this mRNA/protein is a major target in cancer treatment (Daikoku et al., 2006). In light of the findings of these previous studies on *cox-1*, we have concentrated on attempting to inhibit MDR by down-regulating *cox-1* using RNAi technology.

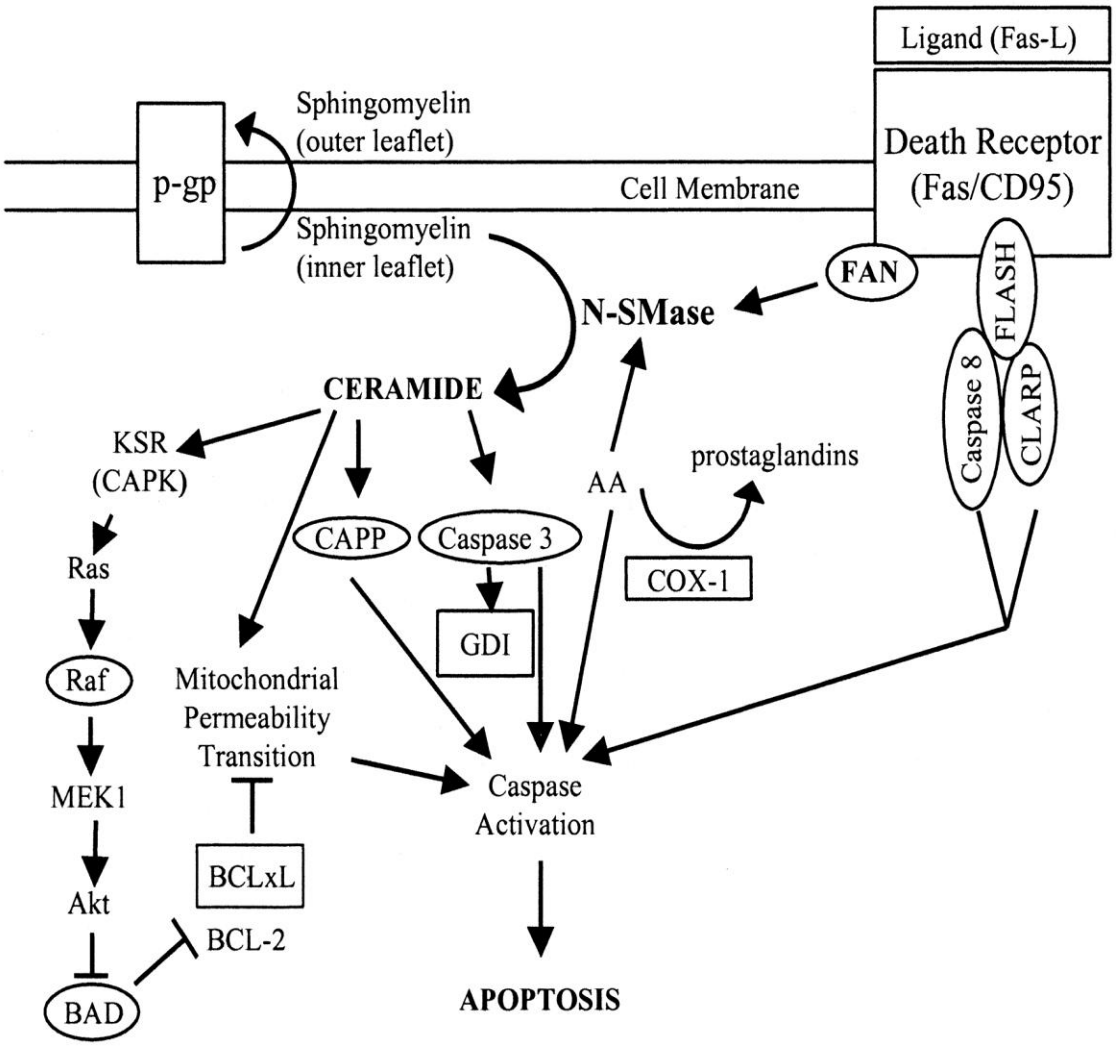


**Fig. 2: Alterations in gene expression observed as a result of doxorubicin selection**. Doxorubicin stimulates ceramide formation, caspase activation, and ultimately apoptosis in many cell types. Increased expression was observed in the genes shown in boxes while the expression was reduced for the genes shown in ovals after doxorubicin selection (George et al., 2001).

# METHODOLOGY

## Cell Lines

The human SCLC cell line with MDR features (GLC4/ADR) was obtained from Dr. Hetty Timmer-Bosscha (University Medical Center Groningen Netherlands) with the help of Ms. Brandy Snider (Indiana University/Purdue University Indianapolis, IN). These cells are resistant to adriamycin (a generic form of doxorubicin) (Schroeijers et al., 2000; Siva et al., 2001). GLC4 was derived from a pleural effusion of a patient with small cell lung cancer and was kept in culture in RPMI 1640 medium plus 10% heat inactivated fetal calf serum (FCS). GLC4/ADR obtained resistance to doxorubicin by stepwise increasing concentrations of doxorubicin (De Jong et al., 1990; Müller et al., 1994). GLC4/ADR is 190.6 ± 16.2 times more resistant to doxorubicin than its parental cell line. The MDR state of the GLC4/ADR cells was attained by treating the GLC4 cells initially with 18 nM ADR. ADR concentration was then doubled after 3 passages with this drug concentration. This procedure was repeated every third passage until an ADR concentration of 1152 nM was reached. After 20 passages at 1152 nM there was no apparent cell death, and the cell line was passed twice a week in growth medium with 1152 nM ADR. The resistance of the GLC4/ADR cell line is dependent on the intracellular level of glutathione (GSH) because pretreatment of the cells with GSH inhibitor substantially reduced resistance (Zijlstra et al., 1986). GLC4 cells grow partly

as loose floating aggregates and partly attached, with a doubling time of 26 h. The cell line has the characteristics of a variant type hSCLC (Zijlstra et al., 1986; Meijer et al., 1990). Three distinct states of these cells can be maintained as GLC4/S (sensitive to doxorubicin), GLC4/ADR (resistant to doxorubicin, MDR), and GLC4/REV (not grown on doxorubicin, exhibiting intermediate characteristics such as fewer membrane pumps and vaults needed to efflux chemotherapeutic drugs. They are capable of rapidly becoming MDR with added doxorubicin).

RPMI medium supplemented with L-glutamine (2 mM), 10% bovine growth serum, and 1% antibiotic/antimycotic (Invitrogen, Carlsbad, CA) was used for culturing the GLC4 cell lines. Cells were maintained in 25 ml tissue culture flasks (Sarstedt Inc., Newton, NC) and were cultured at 37°C and 5% $CO_2$. Doxorubicin was added to growth medium for the GLC4/ADR cells to achieve a final concentration of 350 nM doxorubicin (the highest concentration of doxorubicin that does not kill our cells as determined by Aryal, 2007). Time to change the medium was determined by a pH indicator that induced a color change from pink to orange when waste products began to approach toxic levels, normally every 3-5 days. Change of medium was done by pelleting the cells at 1000 rpm in a bench top centrifuge for 5 min and using a sterile pasteur pipette to aspirate off the used medium. Ten ml of fresh medium was used to resuspend the cell pellet.

For long term storage in liquid nitrogen, 10 ml of a cell suspension was centrifuged at 1000 rpm for 5 min and the pellets were resuspended in 1 ml of a freezing solution [7 parts RPMI, 2 parts bovine growth serum (BGS), and 1 part dimethyl sulfoxide (DMSO)] such that the final concentration was approximately 2-3 x $10^6$

cells/ml. One ml of cell suspension was placed in a cryovial which was transfered to a cooling chamber containing isopropyl alcohol to regulate the rate of cooling to a drop of 1°C/min until the cells were frozen. The cooling chamber was placed in a -80°C freezer overnight and the frozen cryovials were transferred to liquid nitrogen the next day.

To wake up cryogenically stored cells, the frozen cell suspension was thawed using a 37°C water bath. Nine ml of growth medium was added to make a total of ten ml. The mixture was pelleted at 1000 rpm for 5 min and a sterile pasteur pipette was used to aspirate off the sleep mixture. The pellet was resuspended in 10 ml of fresh medium and the solution was placed in a T-25 flask.

### *cox-1* Down-Regulation Using siRNA Technology

A previous study using GLC4/ADR cells obtained from UCLA showed significant up-regulation in *cox-1* expression (Aryal, 2007). However, we obtained a different GLC4/ADR cell line from a European lab and it was necessary to perform a preliminary RT-PCR experiment with *cox-1* specific primers to confirm that *cox-1* was also up-regulated in these cells.

Once we confirmed the over-expression of *cox-1* in our new GLC4/ADR cells, we purchased *cox-1* siRNA for the RNAi experiment (Santa Cruz Biotechnology, Santa Cruz, CA). This was a target-specific 20-25 nt siRNA constructed against mRNA accession #NM_000962. The sequences for the siRNA were: Sense Strand 1-GUGCCAUCCAAACUCUAUCTT and Anti Sense Strand 1-GAUAGAGUUUGGAU GGCACTT, with a G/C percentage of 42.9 %.

Cells were transfected in triplicate in 6-well culture plates containing either GLC4/REV or ADR cells. Cells were plated at 1 x$10^6$ cells/ml and incubated for 24 h

such that on the day of the transfection $2x10^6$ cells/ml was achieved. To achieve the ADR state, doxorubicin of 350 nM was added to the REV cells at the time of plating. One hundred µl of DNA Diluent B from the GenePORTER 2 QuikEase™ transfection kit (Genlantis, San Diego, CA) was mixed with 55 µl of siRNA [10 µM (4µg)] and incubated for 5 min at room temperature (~25°C). This dilution was added to 95 µl of OPTI MEM serum free medium (Invitrogen, Carlsbad, CA) and placed in a QuikEase™ tube to incubate the resulting 250 µl solution for 20 min at room temperature. To the cell culture in each well, 250 µl of stable nucleic acid-lipid particle solution was added. Controls included non-transfected ADR cells and ADR cells transfected with scrambled siRNA (a negative control targeting no known RNA transcript in the human genome) (IDT, Coralville, IA). After 4 h of transfection, an additional 46 µl of OPTI MEM was added to each of the wells. Cells were harvested and analyzed after 24 h, the optimal time to observe the effects of transfection which were expected to last up to 72 h. Transfection efficiencies were compared using different transfection kits (Adam, 2004) and Pratik Aryal determined nearly all cells were transfected using this system with GLC4 cells and BlockiT fluorescent oligo (Aryal, 2007).

**RNA Isolation**

Total cellular RNA was isolated from 500 µl of the transfected cells ($1x10^6$ cells, 1/3 of the total) to confirm *cox-1* knockdown. RiboZol™ RNA Extraction Reagent (Amresco, Solon, OH) was used to extract and purify the RNA following the manufacturer's instructions. Cells were pelleted by centrifugation in an RNase-free tube. The supernatant was discarded following centrifugation and the pellet was resuspended in 1 ml of Ribozol™ RNA Extraction Reagent per $5x10^6$ cells. Washing of the cells was

avoided before the addition of Ribozol™ RNA Extraction Reagent as it would tend to result in the degradation of mRNA. Cells were lysed by passing them several times through the tip of a pipette.

The homogenized sample was incubated for 5-10 min at room temperature to insure the complete dissociation of nucleoprotein complexes. Two hundred µl of chloroform was added per 1 ml of Ribozol™ RNA Extraction Reagent and the tube was tightly secured. The tube was shaken vigorously for 15 s to mix the sample which was then incubated for 2-3 min at room temperature. The sample was centrifuged at 9750 rpm for 15 min at $4^{o}$C using a micro-centrifuge which yielded three phases: a) a lower red, phenol-chloroform phase, b) a white interphase, and c) a colorless, upper, aqueous phase containing the RNA. Only about 80% of the clear upper aqueous phase was carefully removed in order to avoid contamination with protein, DNA, lipids and carbohydrates that appeared as debris or flocculent material at the interface. The remaining 10-20% of the original aqueous phase was back-extracted by adding an equal volume of Ribozol™ RNA Extraction Reagent to the remaining phenol solution. The solution was vortexed and centrifuged to separate the layers. The top aqueous layer was removed as described above and the two aqueous layers were combined.

The pooled aqueous phase was transferred to a new RNase-free tube and the RNA was precipitated by adding 0.5 ml of isopropanol per 1 ml of Ribozol™ RNA Extraction Reagent in the initial homogenization. Samples were incubated for 10 min at room temperature and centrifuged at 9750 rpm for 10 min at $4^{o}$C. A white or gel-like pellet of precipitated RNA was formed along the side and bottom of the tube. The size of

the pellet depended on the amount of cell/tissue starting material but the pellet of purified RNA was nearly transparent and difficult to see.

The supernatant was carefully removed without disrupting the RNA pellet. The pellet was washed with 75% ethanol prepared with RNase-free water. For each wash, 1 ml of ethanol was added per 1 ml of Ribozol™ RNA Extraction Reagent used in the initial homogenization. It was vortexed and centrifuged at 6094 rpm for 5 min at $4^{o}$C.

Following the final ethanol wash, the ethanol was carefully removed without disrupting the pellet. The pellet was briefly air-dried for 5-10 min. However, the pellet was not dried completely as it would decrease the solubility of the RNA. The RNA pellet was dissolved in 50 µl RNase-free water for every $5x10^{6}$ cells or 10 $cm^{2}$ dish. The pellet was passed several times through a pipette tip and incubated for 10 min at 55-$60^{o}$C to permit it to completely dissolve. Finally, the RNA concentration was determined by measuring absorbance at $A_{260}$ and using the following formula: RNA concentration in µg/ml = $A_{260}$ x 40 x the dilution factor.

**RT-PCR Measurement of *cox-1* Expression in GLC4 Cells**

RT-PCR was used initially to confirm the up-regulation of *cox-1* in the new GLC4/ADR cells and also to compare *cox-1* levels in transfected cells. RNA extracted from the cultured cells was quantified as described previously. Superscipt III Platinum SYBR Green One Time qRT-PCR Kit (Invitrogen) was used with extracted RNA as a template. Primers used in these reactions were specific for *cox-1* and were purchased from Santa Cruz Biotechnology. The components for the RT-PCR reactions were as follows: 1 µl of Superscript III RT Mix, 25 µl of 1 X SYBR Green, 1 µl of forward and reverse primers (10 µM each), 1 µg of RNA template (maximum volume 10 µl), 1 mM

magnesium sulfate, 20 ng/µl ultrapure, non-acetylated bovine serum albumin, and molecular grade water to 50 µl.

The Cepheid Smart Cycler (Cepheid, Sunnyvale, CA) was used for the RT-PCR amplification. The standard cycling program was used: cDNA synthesis @ $50^{o}$ C for 3 min; denaturation @ $95^{o}$ C for 5 min, followed by 40 cycles of annealing and extension ($95^{o}$ C for 15 s and $60^{o}$ C for 30 s), and finally $40^{o}$ C for a minute. Comparisons of the change in fluorescence over time were used to analyze the results.

**Cell Viability Assay using Hemacytometer Cell Counts**

In order to perform a cell count using a hemacytometer, approximately 0.2 million cells (1/10 of the total) were stained with trypan blue dye. Under a microscope, live cells appeared clear and transparent whereas, the dead cells appeared blue. The trypan blue stain solution was added to the hemacytometer grid carefully using a coverslip to spread the solution by surface tension. The live cells (clear cells) at four square mm corners of the hemacytometer were counted under the microscope. The average counts of the four square mm corners were used for cell count per square millimeter to determine the cell concentration using the following formula: The number of cells per milliliter = number of cells counted per square millimeter (average of four corners) x dilution x $10^4$; Total cells = cells/ml x total culture volume (ml).

The percentages of viable cells were measured by dividing the number of viable cells by the total cells present in the sample. Both *cox-1 a*nd scrambled siRNAs were used for transfection and percentage of viable cells were compared with the non-transfected and their control group. All the samples were in triplicate and the final

percentage of viable cells was the average of this triplicate. Statistical differences were determined using a paired Student's *t*- test and significance was established when *P <0.05, **P <0.01.

**Apoptosis Assay Using Fluorescence Microscopy**

A multiplex fluorescence apoptosis/necrosis detection kit (Enzo Life Sciences, Plymouth Meeting, PA) was used to determine if apoptosis was restored with transfection. Early apoptosis was detected by the display of phosphatidylserine (PS) on the extracellular face of the plasma membrane. In the presence of $Ca^{2+}$, phospholipid-binding proteins such as annexin-V/FITC bind with a high affinity to PS. Since annexin-V/FITC is not cell permeable, the binding of externalized PS is a strong confirmation of early apoptotic cells.

Detection of early apoptosis was enabled by an annexin-V-EnzoGold (enhanced cyanine-3) conjugate. Similarly, late apoptosis and necrosis detection was facilitated by a Necrosis Detection Reagent (Red) similar to the red-emitting dye 7-AAD. However, we were only able to assess the early apoptosis level using the fluorescence apoptosis/necrosis detection kit since our fluorescence microscope did not have the proper filter set for the necrosis detection.

An apoptosis assay was also performed using propidium iodide (PI) versus annexin-V/ FITC (BD Pharmingen, San Diego, CA) staining to compare the early and late stages of apoptosis. PI is an intercalating agent, with no discernable sequence specificity, which binds DNA at a ratio of 4 bps per molecule PI bound (Riccardi et al., 2006). When PI is excited by laser light at 488 nm its fluorescence is detected between 500-670 nm. The fluorescence is amplified 20-30 fold when PI is bound to DNA, but PI

is impermeable to the cell membranes of viable cells. Once a cell has undergone apoptosis, PI is able to diffuse through the cells and, thus, labeling occurs. Annexin-V/FITC binds to cells early in apoptosis, and continues to be bound through cell death. PI is used in two-color annexin-V/FITC flow cytometric assays to distinguish cells that are in the earlier stages of apoptosis (annexin-V/FITC positive, PI negative) from those that are in the later stages of apoptosis or already dead (annexin-V/FITC positive, PI positive) (Martin et al., 1995).

Cells treated with annexin-V/EnzoGold from the apotosis detection kit and with the two dyes, annexin-V/FITC and PI, were analyzed using Zeiss LSM 5 Pascal fluorescence microscope. These cells included ones transfected with *cox-1* specific siRNA, scrambled siRNA as a control, and untransfected ones. The fluorescence images for the annexin-V/EnzoGold were taken using a filter set at $\lambda_{ex}$ = 550 nm, and $\lambda_{em}$ = 570 nm (400X magnification). Similarly, the images for PI and annexin-V/FITC were taken using a filter set at $\lambda_{ex}$ = 540 nm and $\lambda_{em}$ = 630 nm for PI and at $\lambda_{ex}$ = 488 nm and $\lambda_{em}$ = 520 nm for annexin-V/FITC (400X magnification).

The cell suspension (approximately 0.6 x $10^6$ cells, 1/6 of the total obtained after 24 hr of transfection ) was centrifuged and washed with Phosphate Buffer Saline (PBS) (BioSource, Carlsbad, CA). The cells were resuspended in 10 µl of PBS buffer and transfered into another tube which contained CyGEL (Biostatus, Leicestershire, England) for attaching the non-adherent cells to a slide. The CyGEL and cell suspension mixture was applied on a microscope slide and covered by a coverslip. Since CyGEL liquefies on ice, this microscope slide was transferred to an ice pack and then placed back at room temperature to re-set.

Cells were stained with annexin-V/EnzoGold (enhanced cyanine-3) conjugate (Enzo Life Sciences, PA) and with fluorescein isothiocyanate (FITC), annexin V, and propidium iodide, as per the manufacturer's directions (BD Pharmingen, CA). Dead cells appeared red in color unlike the white live cells after staining was done with annexin-V/EnzoGold. Contrary to this, early apoptotic cells appeared green and late apoptotic cells appeared red in the cells stained with annexin-V/FITC and PI, respectively. The number of dead cells was divided by the total cells to measure the percentage of apoptosis.

**Apoptosis Analysis Using Flow Cytometry**

Transfected cells (500 µl) were harvested from each well of the 6 well plate which approximately contained 0.4 million cells (1/7 of the total). The cell suspension was pelleted at 1000 rpm for 5 min. The supernatant was discarded and the pellets were resuspended in cold PBS. It was repeated one more time with cold PBS. For the dead control, 0.5 million cells were treated with 95 % ethanol while for other samples PBS was added instead of ethanol. It was incubated for 2 min and was followed by centrifugation and pouring off the supernatant. The pellets were resuspended with 250 µl 1x Binding Buffer and 100 µl of the solution was transferred to a FACS tube which was kept on ice. Ten µl of 0.5 mg/ml PI and 10 µl annexin-V/FITC were added to the specified tube which was gently vortexed and then incubated for 15 min on ice in the dark. Finally, 400 µl of 1X Binding Buffer was added to each tube and flow cytometry was performed as soon as possible. Flow cytometry was performed on a COULTER® EPICS® XL-MCL Flow Cytometer (Beckman, Fullerton, CA) to determine the percentage of dead cells in a group of cultured cells (Lecoeur et al., 2002).

**Western Analysis**

In order to determine if there was a simultaneous reduction in the amount of COX-1 protein expressed in transfected cells relative to control cells, a Western analysis was performed by an undergraduate student, Fernando Cuadrado. Total protein from six samples was isolated and analyzed by Western blotting. Two sets of duplicate samples included doxorubicin treated and non-treated cells. Within each set were ADR cells transfected with *cox-1* specific siRNA, cells transfected with scrambled siRNA, and non-transfected cells. The protein isolation was performed using a radioimmunoprecipitation assay or RIPA buffer (Thermo Fisher Scientific, Waltham, MA). During this process, cells were chemically lysed and centrifuged to extract all proteins present at the time of processing. Bradford assay was used to quantify the total amount of protein.

The total amount of protein obtained was highly dependent on the number of cells utilized. For this experiment each replicate sample contained approximately 750,000 cells which were harvested (1/4 of the total of each experimental group). Each group contained a total initial volume of 375 µl with a cell concentration of $2 \times 10^5$ cells/ml. The cells were centrifuged at 2,000 rpm and the supernatant obtained was discarded. The cell pellets were washed twice with 500 µl of cold PBS, by repeating the first step. These were resuspended in 150 µl of RIPA buffer (1 ml per $5 \times 10^6$ cells) and mixed into solution by pipetting up and down several times. The cells were placed on ice followed by incubation on a rocking platform for 15 min. Each sample was centrifuged at 12,000 rpm for 15 min to pellet cell debris. Finally, the supernatant was extracted and protein quantification was performed transferring supernatants to new tubes.

A Bradford assay was performed for quantification. A standard curve was constructed by reading the absorbance values of five standard concentrations containing

1, 2, 3, 4 and 5 µl of bovine serum albumin (BSA) (BioRad, Hercules, CA) at concentration of 1.47 µg/µl to 200 µl of 5X Bradford solution and molecular grade water up to a total volume of 1 ml. A graph for all the standards was done by plotting absorbance as a function of concentration. Table 1 shows the exact components, absorbance values and concentration in the standard curve.

| Bradford solution | Water | BSA µg/µl | Absorbance |
|---|---|---|---|
| 200 | 800 | 0 | 0.1905 |
| 200 | 799 | 1.47 | 0.1905 |
| 200 | 798 | 2.94 | 0.378 |
| 200 | 797 | 4.41 | 0.601 |
| 200 | 796 | 5.88 | 0.7395 |
| 200 | 795 | 7.35 | 0.8 |

**Table 1: Bradford assay standards.** The absorbance of six standards, with increasing BSA concentrations, was measured at 595 nm. A 5X Bradford solution utilized for this assay.

A 1:250 dilution of each protein was made in 996 µl of 5X Bradford solution (BioRad, Hercules, CA) before calculating the total amount of protein in solution. All samples of the same type (the experiment was run in triplicate) were pooled together resulting in a total of six samples to increase the total amount of protein per sample group. Table 2 shows the absorbance values and concentrations after using the equation obtained with the Bradford assay and multiplying by the dilution factor (250).

| Sample | Absorbance (595 nm) | Concentration (µg/µl) |
|---|---|---|
| 1 | 0.424 | 0.8495 |
| 2 | 0.408 | 0.8125 |
| 3 | 0.323 | 0.6325 |
| 4 | 0.266 | 0.5125 |
| 5 | 0.337 | 0.665 |
| 6 | 0.269 | 0.5175 |

**Table 2: Absorbance values (595nm) and concentration for each sample.**

The total amount of protein loaded per lane was normalized to 8 µg for Western analysis. The samples were run in an SDS-PAGE denaturing gel (NuPAGE, Invitrogen, Carlsbad, CA) for 1 hr and 45 min at 150 V. The total volume of each sample was set to 35 µl with addition of varying amount of molecular grade water and 17.5 µl of 2X sample buffer was added to each sample. Table 3 shows the calculated protein sample volumes loaded onto the gel.

Before loading, the samples were boiled for 5 min. A brief centrifugation step was added to reincorporate condensed liquid in the lid. The pre-cast gel was set into a BioRad apparatus and 200 ml of 1X running buffer was added to the inner chamber. After verifying that no bubbles were present in any well, an additional 600 ml was added to the outer chamber.

| Sample | Concentration (µg/µl) | Volume (µl; 8 µg) |
|---|---|---|
| 1 | 0.8495 | 9.42 |
| 2 | 0.8125 | 9.85 |
| 3 | 0.6325 | 12.65 |
| 4 | 0.5125 | 15.60 |
| 5 | 0.665 | 12.0 |
| 6 | 0.5175 | 15.46 |

**Table 3: Protein sample volumes for equal amount of protein per well.** The sample loaded per lane was normalized to 8 µg (Cuadrado, 2010).

A protein molecular weight marker was added to the first and eighth well of the 10-well polyacrylamide gel (10 % gel). Fig. 12 shows the loading order of the samples which duplicated many of the samples on the two sides. The gel was run for at 150 V for 1 hr and 45 min. Following electrophoresis, the gel was cut into two separate portions after the run. Lanes 1-7 were exposed to electrophoretic transfer followed by immunoprecipitation versus COX-1 and actin antibodies and lanes 8-10 were stained with Coomassie blue. The bands in molecular weight markers which were used to determine hybridizing protein were visible in Coomassie blue stained portion.

A semi-dry transfer method from OWL separation systems (ThermoFisher, Waltham, MA) was used in this experiment. Six sheets of blotting filter paper (size of 6.5 cm x 7 cm) were placed in the apparatus and air bubbles were avoided. A "sandwich" was made by first placing the first three sheets soaked in cathode buffer

which were followed by the unstained portion of the polyacrylamide gel into the apparatus. A pre-hydrated (MilliQ® water) nitrocellulose membrane was placed on top of the gel followed by two sheets of blotting paper soaked in anode buffer 2 and the last sheet soaked in anode buffer 1. Table 4 shows the dilutions of all three buffers [anode (1 & 2) and cathode buffers]. Finally, the transfer was run at a constant current of 41 mA (0.9 mA/cm$^2$) for 1 hr and 45 min.

| Buffer 3x (A1, A2 or C) | Distilled water | Methanol |
|---|---|---|
| 330 mL | 470 mL | 200 mL |

**Table 4: Buffer components for a total of 1000 ml 1X working anode, anode1 and/or cathode buffer solution.** Buffers were obtained from OWL separation systems (ThermoFisher, Waltham, MA).

After the transfer, the nitrocellulose membrane was washed in 5 ml of PBS twice before placing it in 3 ml of Odyssey blocking buffer (LI-COR Biosciences, Lincoln, NE) at 4$^o$ C on rocking platform overnight. The following day, the blot was washed with PBS twice before probing it with the primary antibody. The anti-COX-1 rabbit IgG was diluted in 399 µl of water for a 1:400 working dilution (Santa Cruz Biotechnology, Santa Cruz, CA). The primary antibody solution consisted of 400 µl of anti-COX-1 antibody (raised in rabbit), 3 ml of blocking buffer and 3 µl of Tween-20 (PBS/0.1% Tween-20). To act as internal loading control, the rabbit actin antibody was also included in the antibody solution. Actin is a globular protein of approximately 42-kDa which is highly conserved and found in most eukaryotic cells. The membrane was placed on a rocking platform at 4°C overnight.

The membrane was washed 4X for 5 min with PBS/0.1% Tween-20 on a rocking platform at room temperature during the final steps. A 1:30,000 secondary antibody dilution (goat anti-rabbit IgG labelled with fluorescent Alexa Fluor 680 dye) was made by adding 1 µl of Alexa Fluor 680 (Invitrogen, Carlsbad, CA) to a covered Falcon® tube containing 3 ml of blocking buffer and 3 µl of Tween-20 (Blocking buffer/0.1% Tween-20). The blocking buffer/Tween-20/antibody solution was added to the washed membrane and incubated for 1 hr. The membrane was washed 4X for 5 min in PBS/0.1% Tween-20. PBS alone was used for the last two washes.

The Western blot image was obtained using a LI-COR imaging system. The inverted blot was placed on the lower left corner of the scanning surface and was covered with the rubber sheet to avoid any air bubbles. The blot was scanned using the 700 nm channel at an intensity level of 5. After the image was obtained and it was determined that the actin antibody did not cross-react, densitometry was performed on the Coomassie-stained portion of the gel to provide evidence of equal protein loading in the lanes. Band intensities of two lanes (proteins isolated from transfected and non-transfected ADR cells) were compared by drawing boxes of equal area around two regions of the gel. An upper region was scanned where differences in expressed proteins were not expected and a lower region corresponding to the size COX-l should run as determined by comparison to the stained molecular weight marker. The intensity and shape area values are given in Tables 5 and 6.

| Sample | Intensity | Shape area |
|---|---|---|
| 1 (Loading control) | 7.7 | 24.65 |
| 3 (Loading control) | 8.5 | 24.65 |
| 1 (COX-1) | 11.6 | 24.65 |
| 3 (COX-1) | 14.1 | 24.65 |

**Table 5: Band intensity values of Coomassie Stain image.** Shape areas were held constant at 24.65 (858 pixels) for comparison.

| Sample | Intensity | Shape area |
|---|---|---|
| siRNA/doxorubicin | 50.9 | 26.89 |
| ScrRNA/doxorubicin | 92.1 | 26.89 |
| No siRNA/doxorubicin | 147.9 | 26.89 |
| siRNA only | 42.7 | 26.89 |
| ScrRNA only | 41.8 | 26.89 |
| No treatment | 56.7 | 26.89 |

**Table 6: Band intensity values of all six Western analysis samples.** Shape areas were held constant at 26.89 (936 pixels) for comparison.

## RESULTS AND DISCUSSION

### Verification of Up-Regulation of *cox-1* in GLC4/ADR Cells

Before beginning the research project to use RNAi technology to decrease the expression of *cox-1*, it was necessary to ascertain that *cox-1* was over-expressed with the development of MDR in the cells we had recently obtained from Europe. The up-regulation of *cox-1* in GLC4/ ADR cells as compared to GLC4/REV cells was confirmed by RT-PCR. After 24 h of transfection, RNA was isolated from all populations of cells and 1 µg from each sample was used as a template for RT-PCR with primers specific to the *cox-1* gene. Results clearly indicated an up-regulation of *cox-1* cDNA in GLC4/ADR cells as compared to the GLC4/REV cells. These results can be seen in Fig. 3 which clearly shows the higher level of GLC4/ADR mRNA template as indicated by the earlier fluorescence peak at approximately 20 cycles compared to 38. NTC was a blank in this panel. Average cycle threshold (Ct) values for GLC4/ADR and REV cells were 16 and 31, respectively. Ct levels, which correspond to the number of cycles required to exceed background, are inversely related to the number of target molecules available for amplification (*cox-1* mRNA in this case). Ct values less than 29 are strong positive reactions, indicating the presence of abundant template while a Ct value of 30-37 indicates moderate amounts of target, and higher Ct levels indicate minimal amounts of

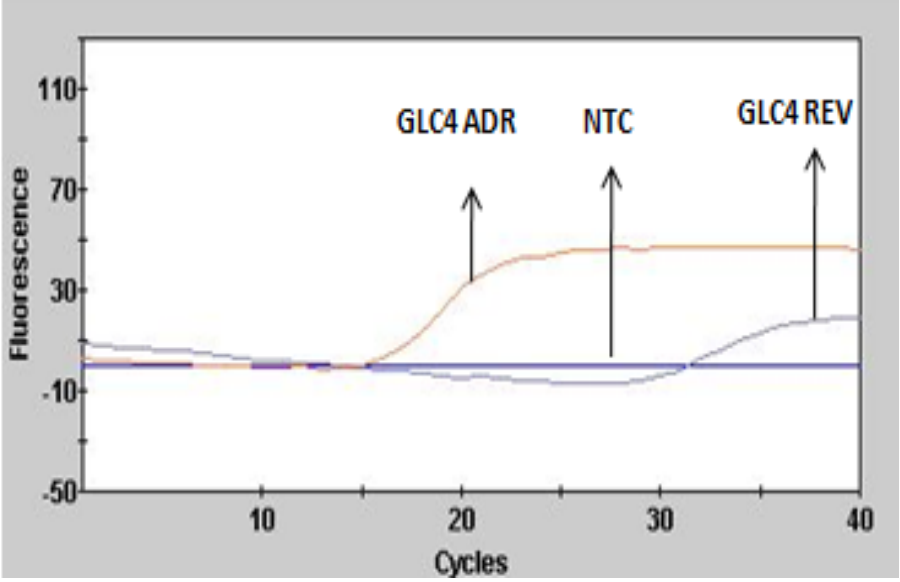


**Fig. 3**: **Real Time RT-PCR amplification of *cox-1* cDNA indicating up-regulation of *cox-1* in GLC4/ADR as compared to REV cells**. Fluorescence curves show the amplification of the *cox-1* cDNA in ADR and REV cells as SYBR green I, an intercalating dye, binds to amplified fragments and releases fluorescence (Y-axis) with increasing cycles of PCR. NTC was a blank in this panel.

target (WVDL, 2010). The results shown here are the best representations from three independent replicates, but indicated that abundant levels of *cox-1* mRNA were present in the ADR cells as compared to moderate to minimal levels in the REV cells. The relative expression level of GLC4/ADR curve was 48 % more than GLC4/REV curve and was based on three sample replicates. We did not perform relative quantification comparing amplification of our target gene transcript to a reference gene transcript and melting curve analysis data could not be retrieved. In addition, we did not include untransfected GLC4/S cells which would have made an interesting comparison. However, in previous research (Aryal, 2007) no significant expression of *cox-1* was observed in GLC4/S cells.

**Down-Regulation of *cox-1* Using RNAi Technology**

Down-regulation of *cox-1* was performed in triplicate using a siRNA specific to *cox-1* and the GenePORTER 2 transfection kit with GLC4/ADR and REV cells grown in 12 well plates. RNA was isolated from each sample after 24 h following addition of siRNA. The total RNA concentration varied from 88 to 176 µg/ml and the range of total RNA isolated was 4.4 to 8.8 µg. In general, GLCR/ADR cells had higher concentrations of RNA compared to GLCR/REV cells which could have been due to a general transcription up-regulation or a specific increase in transcription of a number of MDR related genes, including *cox-1*.

Equal amounts of RNA (1 µg) were used with RT-PCR to compare the levels of *cox-1* expression. The data shown in Fig. 4 confirm the successful down-regulation of *cox-1* in ADR cells transfected with *cox-1* siRNA as compared to non-transfected ADR cells and NTC (a no-RNA control). Results clearly indicated an up-regulation of *cox-1* cDNA in GLC4/ADR cells as compared to *cox-1* down-regulated GLC4/ADR cells.

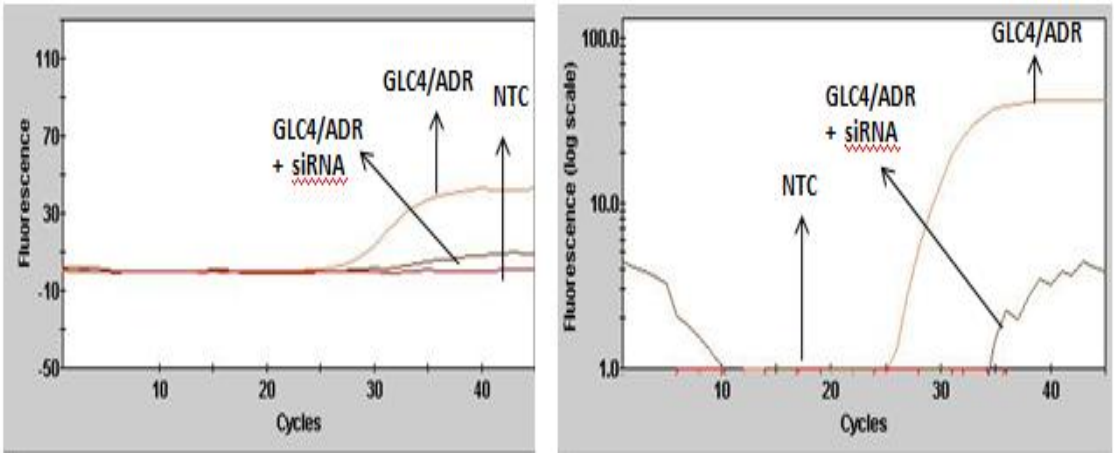


**Fig. 4**: **Real Time RT-PCR amplification of *cox-1* cDNA indicating successful down-regulation of *cox-1*.** Panel A shows the amplification of the *cox-1* cDNA in ADR cells as measured by increased fluorescence (Y-axis) with increasing cycles of PCR. The level of *cox-1* expression is clearly reduced in ADR cells transfected with *cox-1* siRNA compared to non-transfected cells. NTC is a no-RNA control. Panel B shows the fluorescence in log scale (Y-axis) versus the number of PCR cycles on the X-axis.

These results in Fig. 4 clearly show the higher level of GLC4/ADR mRNA template as indicated by the earlier fluorescence peak at approximately 25 cycles compared to 32 cycles. Average cycle threshold (Ct) values for GLC4/ADR and transfected GLC4/ADR cells were 23 and 34, respectively. The results shown here are the best representations from three independent replicates and indicate the presence of abundant levels of *cox-1* mRNA in the ADR cells to moderate levels of *cox-1* mRNA in the transfected ADR cells. The relative expression level of GLC4/ADR curve was 33 % more than transfected GLC4/ADR curve and was based on three sample replicates. We did not perform relative quantification comparing amplification of our target gene transcript to a reference gene transcript and melting curve analysis data could not be retrieved.

**Cell Viability Assay Using a Hemacytometer**

Cell viability was assayed by counting cells in the presence of trypan blue with a hemacytometer. Dead cells appeared blue in color unlike live cells which were colorless. The percentage of viable cells for different populations of cells is shown in Table 7 below. Both *cox-1* and a scrambled (SD) siRNA were used for transfection and the percentage of cell viability was compared with non-transfected cells.

The same results are shown in Fig. 5 in the form of a histogram of mean values with the standard deviations (±s.d.) from three independent experiments. The corresponding P values (*= $P < 0.05$ for ADR cells and **= $P < 0.01$ for REV cells, respectively) showed that there was a significant decrease in cell viability percentage after *cox-1* down- regulation in both the ADR and REV cells. This significant decrease in cell viability percentage in transfected ADR cells is believed to result from the cells'

susceptibility to doxorubicin after down-regulation of *cox-1*, which according to our hypothesis is the target gene responsible for MDR development.

| Cell Viability (%) | | | | |
|---|---|---|---|---|
| REV+No siRNA | REV+siRNA | ADR+No siRNA | ADR+SD | ADR+ siRNA |
| 91.4 | 83.7 | 78.5 | 80.0 | 75.6 |
| 92.1 | 84.2 | 79.8 | 77.9 | 73.3 |
| 91.1 | 83.3 | 80.2 | 78.0 | 74.8 |
| Mean=91.5 | Mean=83.7** | Mean=79.5 | Mean=78.6 | Mean=74.6* |

**Table 7**: **Cell viability assay using a hemacytometer cell count and trypan blue dye to compare the percentage of viability for different populations of cells from three replicate samples.** Both *cox-1* and a scrambled (SD) siRNA were used for transfection. *cox-1* down-regulation induced a significant decrease in percentage of cell viability for both GLC4/ADR and REV cells compared to non-transfected cells or cells transfected with scrambled siRNA (**= $P < 0.01$ for REV cells and * = $P < 0.05$ for ADR cells).

The decrease in cell viability percentage in transfected REV cells not grown in the presence of doxorubicin is more difficult to explain. REV cells are ADR cells grown without doxorubicin which are quickly able to develop MDR in the presence of the drug. REV cells are genetically different from S cells which have not been exposed to doxorubicin. We do not know what specific genetic changes differentiate ADR cells from S cells. However, one previous study suggested that resistance of the GLC4/ADR cell line is dependent on the intracellular level of glutathione (GSH) because pretreatment of cells with GSH inhibitor substantially reduced resistance (Zijlstra et al., 1986).

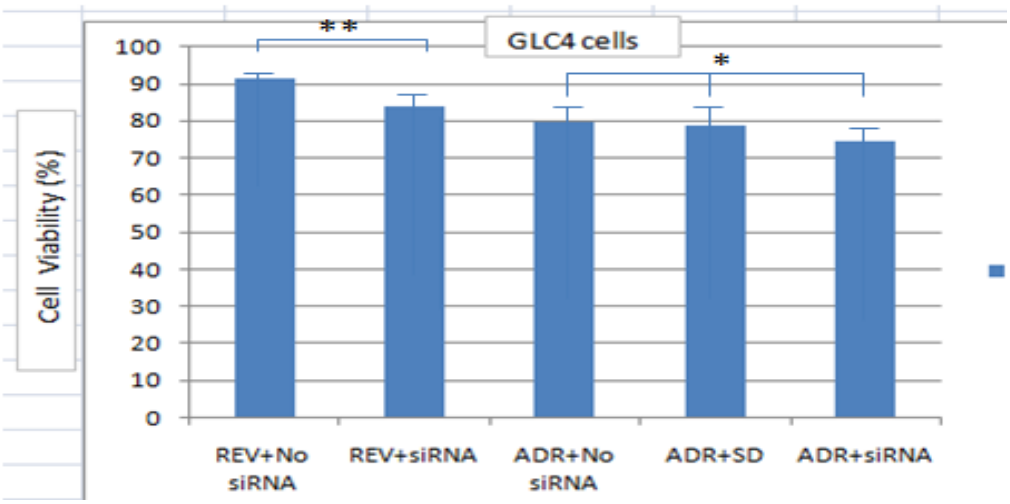


**Fig. 5**: ***cox-1* down-regulation decreased viability in GLC4 ADR and REV cells.**

Percentage of cell viability was measured using a hemacytometer to count cells in the presence of trypan blue dye where dead cells were blue in color compared to the colorless live cells. Both *cox-1 a*nd scrambled siRNAs (control siRNA) were used for transfection. The different populations of cells are shown on the X-axis while the percentage of cell viability is on the Y-axis. A significant decrease in percentage of cell viability was observed after *cox-1* down-regulation in GLC4/ADR and REV cells. Data shown represent the mean ±s.d. of three independent experiments (*= P <0.05, ** = P <0.01).

REV cells are known to have an intermediate number of vaults present compared to S and ADR cells and it is likely that they also contain more *cox-1* mRNA. Previous research in our lab (Aryal, 2007) reported intermediate levels of *cox-1* mRNA and COX-1 protein activity in REV cells as compared to ADR cells. Therefore, it is assumed that decreasing *cox-1* expression in REV cells in this research also negatively impacted these cells.

We also found that there was slightly lower percentage of viability (not significant) in the cells treated with scrambled siRNA as compared to the non-transfected cells suggesting all siRNAs are slightly toxic to the cells as previously observed by Fedorov et al. (2006).

**Assessment of Apoptosis Using Fluorescence Microscopy**

Since our cells were a mixed population of cells that were not all adherent, GLC4/REV and ADR cells transfected with *cox-1* siRNA, a scrambled siRNA, and the untransfected cells were fixed on glass slides with Cygel (Biostatus Limited, Leicestershire, United Kingdom). A Zeiss LSM 5 Pascal fluorescence microscope and a fluorescent apoptosis/necrosis detection kit (Enzo Life Sciences, PA) were used for taking fluorescence images which showed increase in percentage of apoptosis after successful down-regulation of *cox-1* from GLC4 cells.

Fig. 6 shows REV cells in panels A and B where only cells in panel B are transfected with *cox-1* siRNA. Panels A and B clearly differentiate the early apoptotic cells (red) from the live cells which are clear and transparent. Red background fluorescence was also detected which is believed to be due to Cygel (Aryal, 2007). The percentage of apoptosis was calculated by dividing the dead cells by the total cells

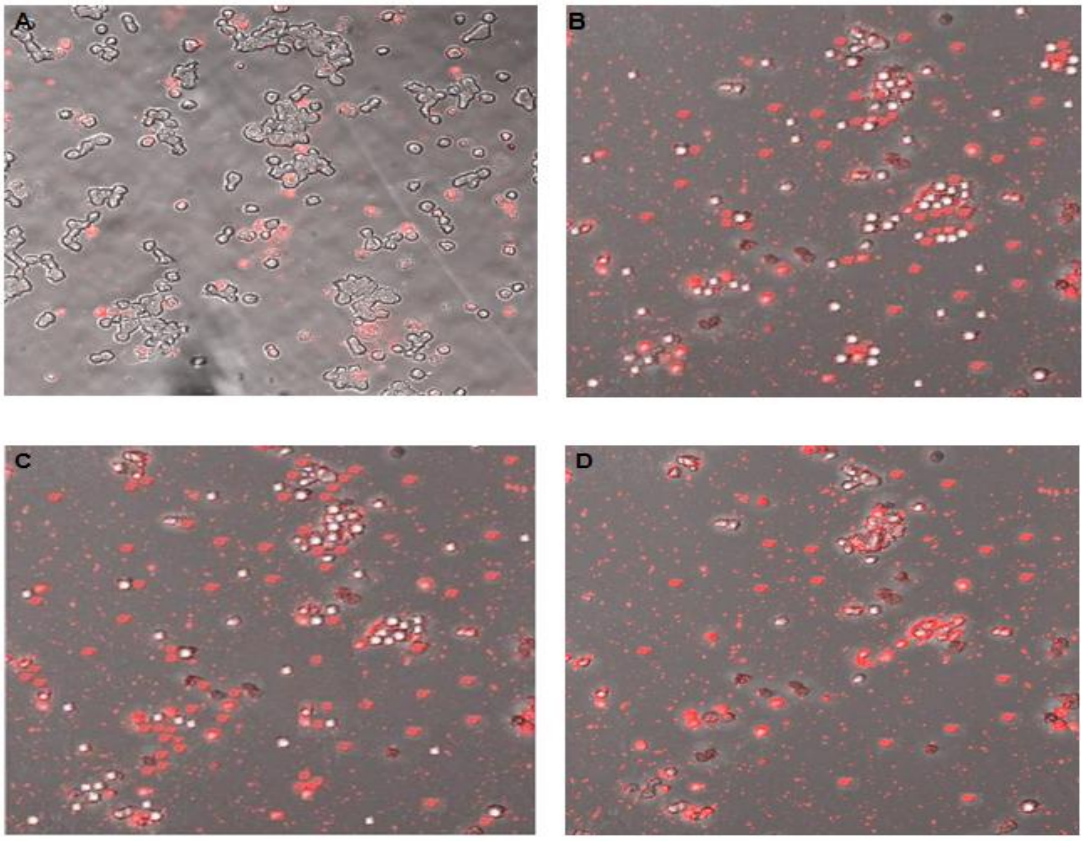


**Fig 6: Annexin-V/EnzoGold conjugate and fluorescence microscopy enabling detection of early apoptosis in REV (Panels A and B) cells and in ADR (Panels C and D) cells.** Early apoptosis is shown by red cells while the live cells are clear and transparent using a fluorescent apoptosis/necrosis detection kit (Enzo Life Sciences, PA). Images were taken with a Zeiss LSM 5 Pascal fluorescence microscope using a filter set at $\lambda_{ex}$ = 550 nm, and $\lambda_{em}$ = 570 nm (400X magnification). Panels A and B contain REV cells but only panel B is transfected with *cox-1* siRNA. A lower percentage of apoptosis (21.1%) was seen in panel A as compared to panel B (48.6%). Panels C and D contain ADR cells. *cox-1* is down-regulated in cells shown in panel C which exhibited a lower percentage of apoptosis (56.7%) compared to panel D (69.4%).

counted and multiplying by 100 to yield a percentage value. A significantly lower percentage of apoptosis (21.1%) was observed in Panel A as compared to panel B (48.6%) which suggests that siRNA treatment to decrease *cox*-1 expression doubled the number of cells experiencing apoptosis. Overall, these apoptosis values were higher than the hemacytometer cell counts where the differences between untransfected and transfected non-viable REV cells again doubled but were only 8.5 % and 16.3 %. This increase in the cell death with the fluorescence assay could be attributed to detrimental effects of the staining procedure or to longer duration of time while preparing the slides. Pre-fixation of the slides may have prevented additional apoptosis. In both assays statistical significance was measured using Student's paired *t*- test (*= $P < 0.01$) to show significant differences between non-transfected and transfected cells and confirm siRNA treatment significantly increased percentage of apoptosis even in REV cells.

Panels C and D show ADR cells. Although *cox-1* down-regulation in REV cells doubled the level of apoptosis and significantly increased the level of apoptosis in ADR cells, a much greater level of apoptosis was seen in both non-transfected and transfected ADR cells. Again, none of the slides were fixed and slides for ADR cells were prepared after finishing the slide preparation for REV cells. These values for apoptosis were also higher as compared to the hemacytometer cell count where untransfected and transfected ADR cells had totals of 20.5 % and 25.4 % non-viable cells. Again, this could be due to longer time and more manipulation required to prepare the slides as compared to performing the hemacytometer cell counts. Thus, these results suggest that the slides should immediately be fixed on the day of preparation.

Fig. 7 shows annexin-V/FITC and propidium iodide staining in ADR cells

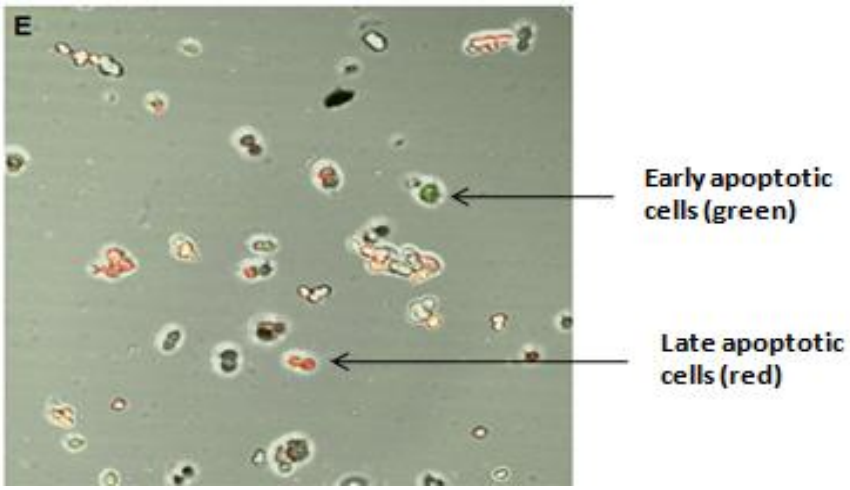


**Fig 7: Apoptosis assay using annexin-V/FITC and propidium iodide (PI) to compare early apoptosis and late apoptosis, respectively, in *cox-1* transfected ADR cells by fluorescence microscopy.** The images were taken using the filter set at $\lambda_{ex}$ = 540 nm, and $\lambda_{em}$ = 630 nm for PI and the filter set at $\lambda_{ex}$ = 488 nm, and $\lambda_{em}$ = 520 nm for annexin-V/FITC (400X magnification). Early apoptosis is shown by green cells while cells in a late stage of apoptosis are red. The slide was chosen because it clearly showed early and late apoptotic cells, but was not representative of the proportion of each counted.

transfected with *cox-1* siRNA to evaluate the proportion of early apoptotic cells (green) versus late apoptotic cells (red). More cells were observed in the late apoptotic stage (30) as compared to those in early apoptosis (14) and the total percentage of apoptosis (78.6%) was higher than the control. Due to the low number of cells counted, no statistics were performed. The control in this case was non-transfected ADR cells (Panel C). Percentages of apoptosis were determined from the average of the two slides. However, cells were counted in just one field of view which had a total of 44 cells. In order to get statistically significant results more than one field of view would have to be counted to increase the total number of cells (>100) and immediate fixation of cells is also advised.

Fig. 8 summarizes the fluorescence results in the form of a histogram and includes the means ±s.d. of three independent replicates, where appropriate. Both *cox-1* and a scrambled siRNA were used for transfection and the percentage of apoptosis was compared with non-transfected cells. Although significant increase in apoptosis were observed in both REV and ADR transfected cells compared to the non-transfected REV and ADR cells, we observed a slightly higher percentage of apoptosis in the transfected ADR cells treated with annexin-V/FITC and PI dyes (Panel E) as compared to the same batch of transfected ADR cells treated with the apoptosis detection reagent. Panel D and E contain the same batch of transfected GLC4 ADR cells but differ in the type of dyes used. Panel E contains annexin-V/FITC and PI dyes for the detection of both early and late stage apoptosis while panel D contains annexin-V/Enzogold for the detection of apoptosis only. A slightly higher percentage of apoptosis in Panel E could be due to a longer time required for the preparation of the fluorescence slides involving two dyes

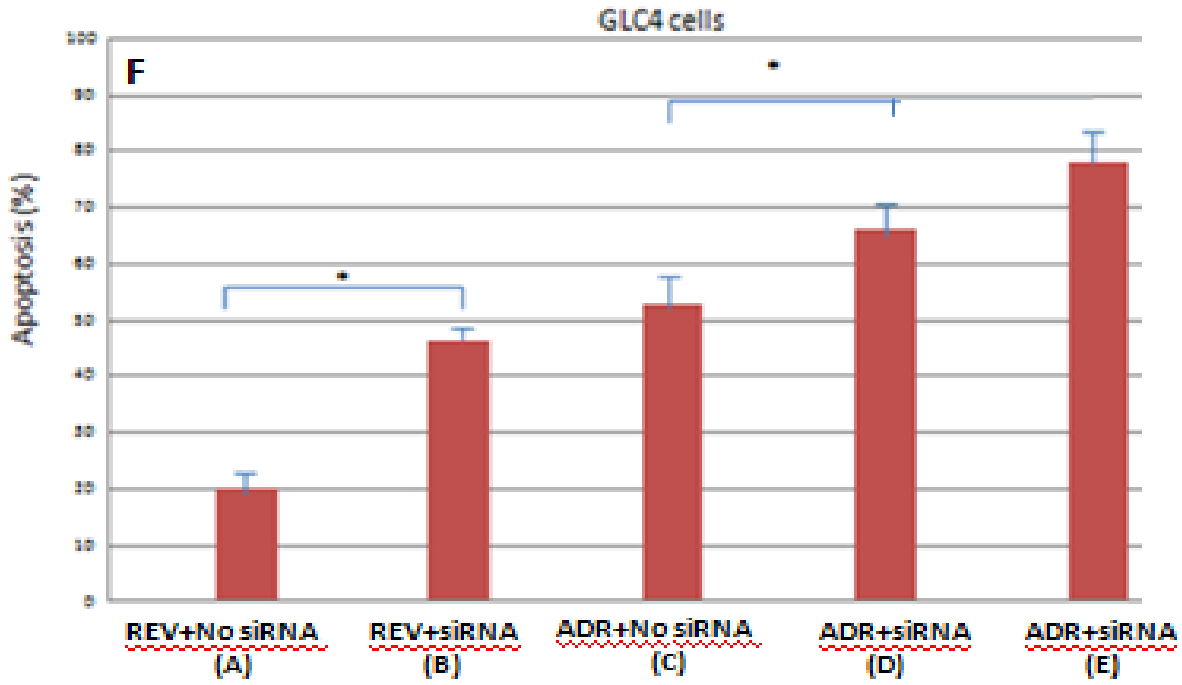


**Fig. 8**: **A histogram comparison of the percentage of apoptosis for transfected and non-transfected REV and ADR cells based on fluorescence data shown in Fig. 8, panels A-E, respectively.** A significant increase in apoptosis was observed after *cox-1* down-regulation in GLC4/REV and ADR cells. The different populations of cells are shown on the X-axis while the percentage of apoptosis is on the Y-axis. Both *cox-1 a*nd scrambled siRNAs (control siRNA) were used for transfection. Panels D and E contains the same batch of transfected GLC4 ADR cells. However, panel D contains annexin-V/Enzogold dye for the detection of apoptosis only contrary to Panel E which contained annexin-V/FITC and PI dyes for the detection of both early and late stage apoptosis. Data shown represent the mean ±s.d. of three independent replicates (*P <0.05).

namely annexin-V/FITC and PI dyes as compared to Panel D which involved only adding the apoptosis detection reagent. None of the slides were fixed that day. The slide in Fig. 7 (Panel E) was the last slide to be made that day which also could have resulted in slightly more dead cells as compared to the cells in (Panel D). This could be solved by fixing the slide using fixative agents such as paraformaldehyde.

**Apoptosis Assay Using Flow Cytometry**

Cells were analyzed 24 h after transfection and apoptosis was assayed with a COULTER® EPICS® XL-MCL Flow Cytometer (Beckman, Fullerton, CA). First, controls were run to test the ability of the flow cytometer to assess apoptosis in our cells. Non-transfected REV cells treated with 95% ethanol to kill them were assayed in the presence of both dyes, annexin-V/FITC and PI, to detect the early and late apoptosis, respectively. FITC conjugated annexin-V binds to phospholipid phosphatidylserine (PS) which is translocated from the inner to the outer leaflet of the plasma membrane in early apoptotic cells, whereas cells should be permeable to PI in late apoptosis due to loss of plasma membrane integrity. Despite repetition of the flow analysis a few times with 50 µg/ml PI (20 times the normal concentration of 2.5 µg/ml) in 100 µl (0.4 million cells), no significant amount of PI was taken up by the cells. The cells picked up the annexin-V/FITC as seen in the lower left quadrant of Fig. 9, but flow cytometry was not showing a majority of dead cells. The results shown in panels A-C in Fig. 9 are difficult to analyze. A large number of dead cells in late apoptosis were expected after treatment with ethanol which would be visible as dots in the upper right quadrant, but this was not observed. We consulted with Dr. Heather Bruns and she suggested that our cells may have been dead before ethanol treatment but we knew this was not the case based on our

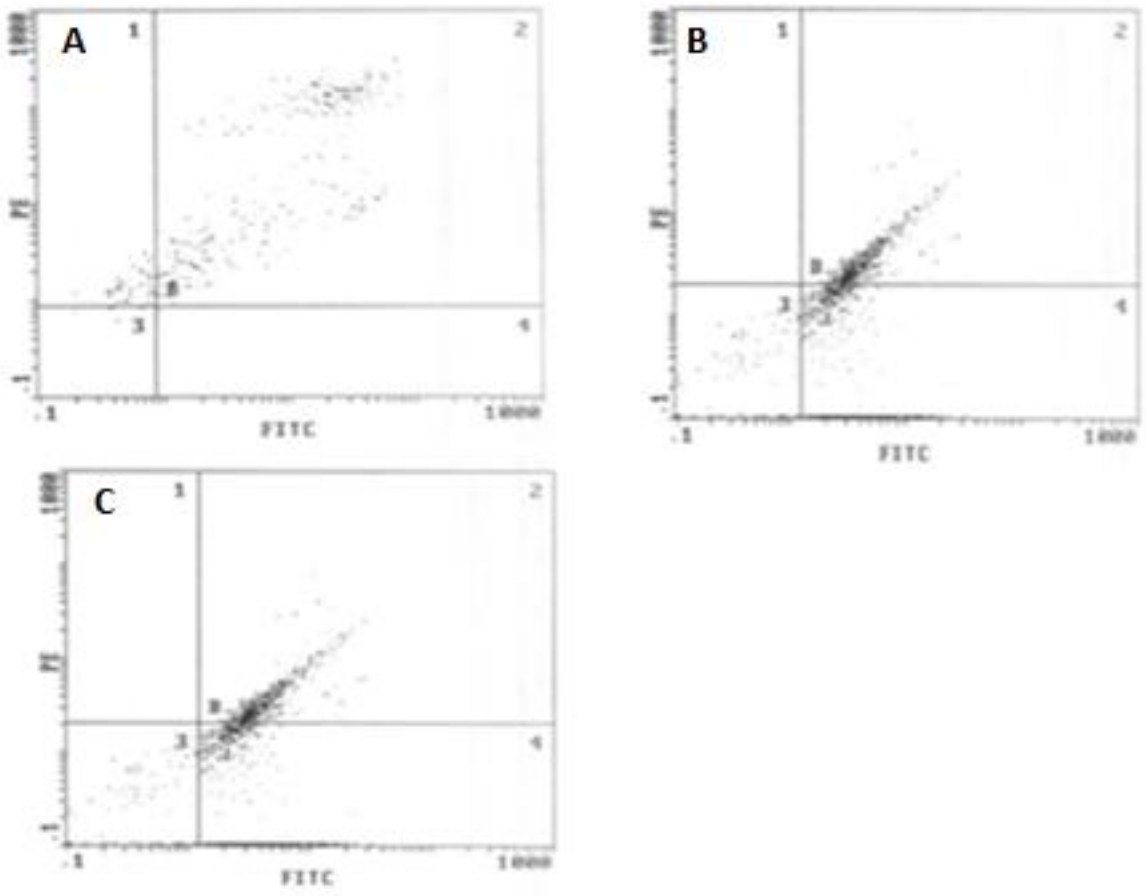


**Fig. 9: Flow cytometric analysis of non-transfected GLC4 REV cells.** Panels A-C are REV cells treated with 95% ethanol in the presence of both dyes, annexin-V/FITC and PI. Cells were expected to take up the dyes in these controls which would be indicated by fine dots in the lower and upper right quadrants representing a greater percentage of apoptotic cells.

other results. Another possibility was that the flow cytometer was not able to distinguish between the two types of cells in our population (adherent and suspension). Dr. Bruns suggested to have the dead control analyzed in a new flow cytometer (from Accuri, Ann Arbor, MI) which was demonstrated in our department.

The new flow cytometer from Accuri was present only one day for a short demonstration and we were allowed to analyze only the dead control experiment (non-transfected REV cells treated with 95 % ethanol). The results of this analysis clearly showed two separate peaks for PI and annexin-V/FITC reflecting the mixture of adherent and suspension cells, which is a characteristic of GLC4 cells in culture (Fig. 10). The resulting data are expressed as 14.5 % annexin-V/FITC positive and PI-negative cells (early stage of apoptosis) in the lower right quadrant and as 83.2 % annexin-V/FITC positive and PI-positive cells (late stage of apoptosis) in the upper right quadrant. Seeing most of the cells in late apoptosis was an expected finding. Unfortunately, we could not compare flow cytometric data with fluorescence microscopy data since treated samples were not run. Thus, we concluded that flow cytometric analyses using our older machine were not possible since this instrument was incapable of distinguishing the two different populations of cells present. If flow cytometry is to be used as a measure of apoptosis in future experiments, a new flow cytometer would be required.

**Down-Regulation of COX-1 Protein Using Western Analysis**

In his thesis research Aryal (2007) showed that the level of COX-1 protein activity (using an enzyme assay) was specifically and significantly decreased from 45.5 to 25.1% after the down-regulation of *cox-1* RNA in GLC4/ADR cells as compared to a non-transfected control. For this experiment we used a Western analysis to confirm

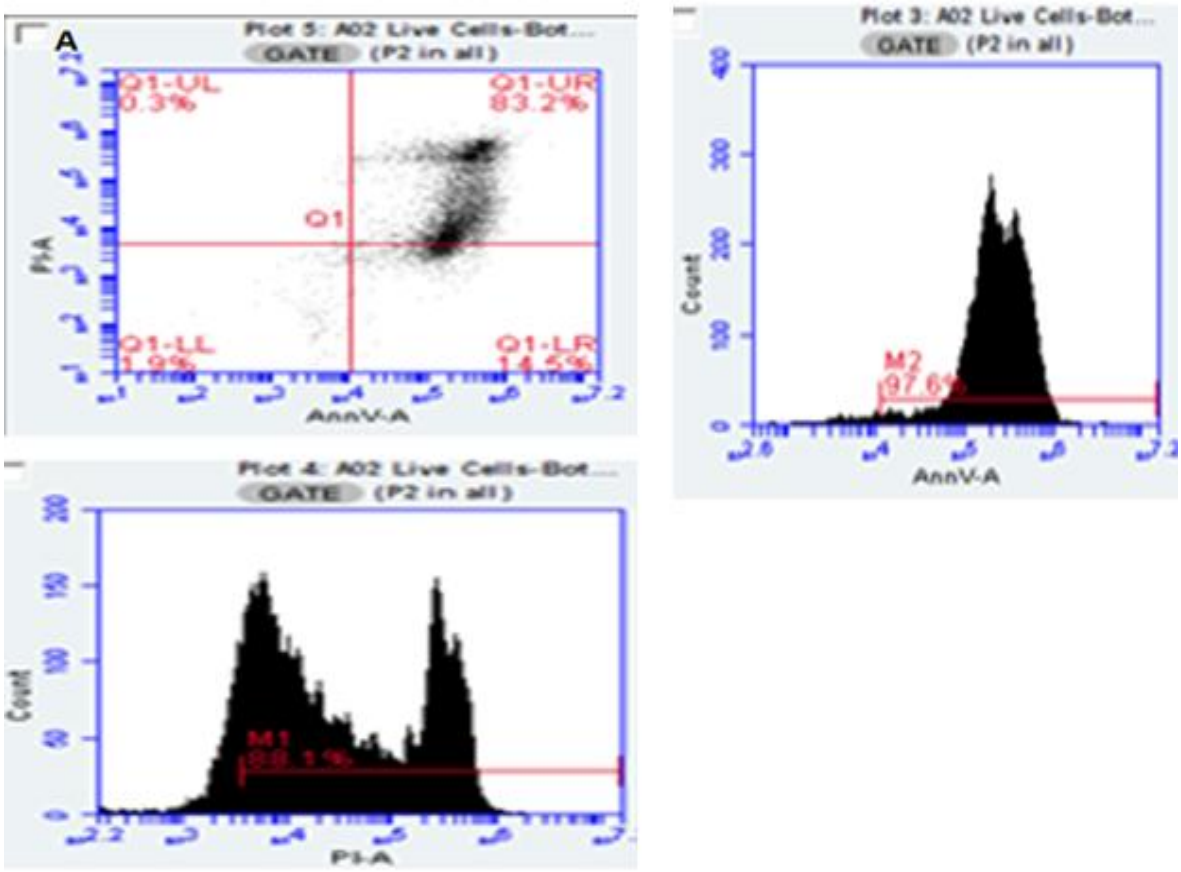


**Fig 10: Flow cytometric analysis using PI and annexin-V/FITC staining of non-transfected REV cells on Accuri Flow Cytometer.** Panel A contains REV cells treated with 95% ethanol in the presence of both dyes, annexin-V/FITC and PI. Two separate peaks for PI and annexin-V/FITC are clearly visible, reflecting the mixture of adherent and suspension cells characteristic of GLC4 cells in culture. Early apoptotic cells (annexin-V/FITC positive, PI negative) observed in the lower right quadrant made up 14.5 % of the total and late apoptotic cells shown in the upper right quadrant made up the remaining 83.2% (annexin-V/FITC positive, PI positive).

down-regulation of COX-1 protein after the siRNA transfection. Following electrophoresis, the acrylamide gel was cut into two separate pieces, one for electrophoretic transfer followed by immunoprecipitation (Fig. 12) and the other one for Coomassie staining (Fig. 11).

Western blot analysis in Fig. 12 shows only the COX-1 protein bands because actin antibody did not cross react. We know this based on the molecular weight marker which is not shown here. If actin antibody had worked, we would have observed one extra band corresponding to actin (42 kDa) below COX-1 (70 kDa) in Fig. 12. Since it lacked an internal control, densitometry was performed on the stained portion in two regions of the gel to confirm equal loading of our samples (Fig. 11). The stained portion was scanned using a LI-COR scanner and a picture is shown in Fig. 11. Two lanes are shown, lane 1 (transfected ADR) and lane 2 (untransfected ADR). The stained molecular weight markers are not shown. To insure equal loading, we performed densitometry using a rectangular box of the same area, 24.65 (858 pixels) in both lanes in two different regions of the gel (Fig 11). First two boxes were placed over the upper regions of the gel where the proteins were not expected to differ. The intensity values for samples 1 and 3 were 7.7 and 8.5, respectively, (a difference of 9.4%) suggesting that total protein loading was nearly equal. Boxes were also placed in the lower region of the gel overlaying bands which corresponded in size to the COX-1 protein. Intensity values in sample 1 and 3 were 11.6 and 14.1, respectively, (an 18% decrease in this region of the gel expected to include COX-1 compared to the non-transfected control). Table 5 shows the band intensity values with a constant shape area for the Coomassie stain image.

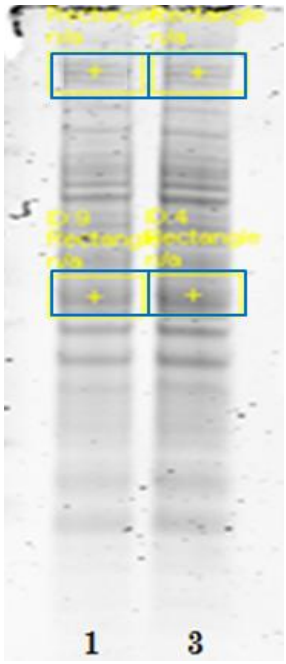


**Fig. 11: Coomassie stained polyacrylamide gel.** Lane 1 contains protein extracts from siRNA- treated GLC4/ADR cells. Lane 3 contains extracts from non siRNA treated GLC4/ADR cells. The boxed areas were held constant at 24.65 (858 pixels) and densitometry was performed for comparison. The intensity values for the upper two boxes in lanes 1 and 3 were 7.7 and 8.5, respectively. The lower two boxes correspond to specific bands in the region of the gel where COX-1 is found. Intensity values for lanes 1 and 3 were 11.6 and 14.1, respectively. Protein standards were run in a separate lane which is not shown here (Cuadrado, 2010).

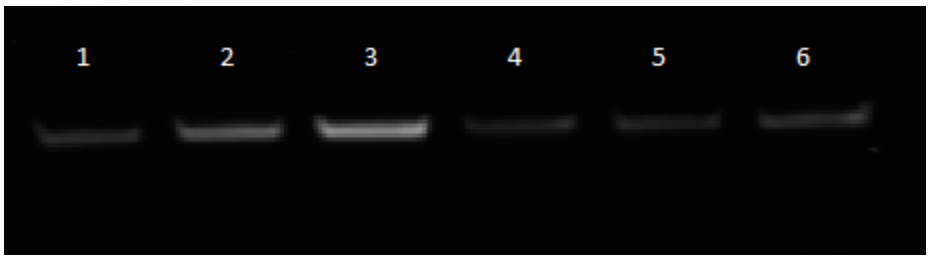


**Fig. 12: Western Blot**. Lane 1, *cox-1* siRNA treated GLC4/ADR cells. Lane 2, scrambled siRNA treated GLC4/ADR cells. Lane 3, non- siRNA treated GLC4/ADR cells. Lane 4-6, same siRNA treatments as in lanes 1-3 with no doxorubicin (Cuadrado, 2010).

.

Similar down-regulation of expression of COX-1 was observed in the portion of the gel subjected to immunoprecipitation (Fig 12). Samples 1-3 contain protein extracts of ADR cells. Lane one contains *cox-1* siRNA transfected cells, lane 2 contains proteins from the scrambled siRNA transfected cells, and proteins from non-siRNA treated cells are shown in lane 3. Lanes 4-6 contain protein extracts from similarly treated REV cells. The level of COX-1 expression appeared to be lower from GLC4/REV cells as compared to GLC4/ADR cells. siRNA transfection in REVcells did not result a significant reduction in COX-1 expression as its level was already very low but differences in intensity were observed in ADR protein extracts. The band in lane 3 (non-transfected) is much more intense than band 1 (transfected). Table 6 shows the band intensity values with a constant shape area for all the six samples.

The findings on Fig. 12 were confirmed by band analysis. For ADR protein extracts, the relative density (COX-1 expression) seen in lane 1 was almost one-third of the COX-1 expression in lane 3. Therefore, results indicated that upon siRNA and doxorubicin treatment, there was an approximately sixty six percent (66%) reduction in COX-1 expression as compared to protein extracts from non-siRNA/doxorubicin treated cells. This reduction (66%) in COX-1 protein expression was greater than that observed by Aryal (DATE) who reported a 44.7 % reduction as determined from a COX-1 protein activity assay. Although only an 18 % difference in the amount of COX-1 protein was apparent from densitometry performed on the Coomassie stained gel as compared to a 66 % down-regulation obtained from immunoprecipitation method, the immuno-precipitation data is stronger. Antibody binding is strong and specific, but Coomassie stain binding with proteins varies widely due to its affinity for proteins rich in basic

amino acids such as arginine, histidine, and lysine. In addition, the densitometry was performed over a region of the gel containing numerous proteins but the immunoprecipitation illuminated only COX-1. A slight decrease in COX-1 expression was also observed upon scrambled siRNA treatment which confirmed that siRNAs generally are slightly toxic to cells, as observed by Fedorov et al. (2006). The band analysis also revealed important information about cells untreated with doxorubicin. Band intensity levels of all samples were compared among each other. GLC4/REV cells without any siRNA treatment (lane 6) showed a slightly higher band intensity value as compared to the values in lanes 4 and 5. Table 6 shows the band intensity values of all the samples.

Hence, Western analysis confirmed that siRNA transfection resulted in decreased expression of COX-1 protein in transfected ADR cells as compared to the non-transfected control, thus supporting other results obtained from cell counts and fluorescence microscopy. However, the lack of a true internal control such as actin detection by immunoprecipitation suggested that the Western analysis should be repeated in the future.

# CONCLUSIONS

Previous studies have shown that *cox-1* is up-regulated in a number of MDR cancer cells such as ovarian and lung cancers. The importance of *cox*-1 has also been suggested by the use of SC-560, an experimental drug which selectively blocks *cox-1*, and resulted a reduced cell proliferation and accelerated apoptosis in ovarian tumors of mice (Daikoku et al., 2005). Although several studies have examined the role of *cox*-2 in MDR (Sorokin et al., 2004), no previous studies have assessed the role of *cox-1*. However, because of a similar role in the induction of inflammation of the COX enzymes and since *cox-1* is up-regulated in GLC4 cells, we decided to examine the effect of down-regulating *cox-1* expression on MDR.

Strong evidence suggesting a close association between COX inhibitors (NSAIDs such as aspirin) and a reduction in colorectal cancer proliferation was shown by Ulrich in 2004. The use of NSAIDs was also linked to protective effects against lung cancers (Olsen et al., 2008). These previous reports clearly suggest that *cox-1* expression is an important target in cancer research because it is now well known that chronic inflammation leads to cancer and inhibiting COX-1, an enzyme with a key role in inflammatory response, should inhibit the cancer growth and proliferation. Although the role of *cox-1* in MDR is not as well documented, our finding that *cox-1* expression increased with the development of MDR in SCLC made it a target of this research.

Our results have shown that concomitant with *cox-1* down-regulation using siRNA, MDR is abolished. RT-PCR amplification of *cox-1* cDNA indicated a successful down-regulation of *cox-1* mRNA following siRNA transfection. *cox-1* siRNA-transfected GLC4/ADR cells had the lowest level of *cox-1* expression when compared to non-transfected GLC4/ADR and REV cells indicating successful *cox-1* down-regulation. After this down-regulation of *cox-1,* a significant increase in apoptosis was suspected as MDR cells became more susceptible to doxorubicin. In addition, a cell viability assay was done using hemacytometer cell counts to show enhanced sensitivity of transfected cells to doxorubicin. Similarly, an apoptosis assay was done using fluorescence microscopy which showed a significant increase in percentage of apoptosis after *cox-1* down-regulation. The greatest increase in apoptosis was observed in transfected ADR cells which originally over-expressed *cox-1*. This significant increase in apoptosis is believed to be due to down-regulation of the inflammatory gene, *cox-1,* as a result of enhanced susceptibility of GLC4/ADR cells to doxorubicin. However, the apoptosis assay using PI and annexin-V/FITC staining during flow cytometry was inconclusive since our flow cytometer was not capable of analysing the GLC4 mixed cell population (adherent and suspension cells).

To confirm these findings at the protein level, an undergraduate student (Fernando Cuadradro) performed a Western blot analysis on a portion of these cells. Fernando found that siRNA transfection decreased the expression of COX-1 by 66% in GLC4/ADR cells as compared to the non-transfected control using densitometry. However, it is recommended that Western blot analysis be performed again. Although densitometry was used on the Coomassie-stained portion of the gel to indicate

approximate equal loading of protein extracts a true internal control such as simultaneous actin immunoprecipitation is needed.

These transfections were performed using siRNA, rather than shRNA, so that the effects were temporary. This provides an advantage in that the genome is not permanently altered. Permanent knock down of *cox-1* is not desired because *cox-1* is a pro-inflammatory gene and if *cox-1* is permanently knocked down, then wounds and infection would never be healed. Although too much inflammation may be detrimental by stimulating cellular transformation and leading to MDR as suggested by this research, inflammation is a needed protective attempt by the organism to remove the harmful stimuli and to initiate the healing process. The use of transient transfection using siRNA allows a rapid analysis of the gene function, since cloning is not required. It allows screening for the cellular response in a quick and inexpensive fashion.

If this experiment is repeated in the future, a better measure of apoptosis is needed. If our department does not purchase a newer flow cytometer, a tunel assay may be performed. Also, other protein such as BCLxL which has been found to be up-regulated in MDR cancer cells could be studied to get a broader insight into factors influencing apoptosis in this cell line. The amount of RNA down-regulation could be quantified using qRT-PCR with a reference gene analysis.

However, all the results confirm that *cox-1* mRNA and protein were down-regulated in transfected GLC4/ADR cells and that apoptosis increased as compared to the controls; a potentially exciting finding for treatment of multi-drug resistant cancer. In the future, a similar experiment could be performed *in vivo* using a mouse model exhibiting MDR lung cancer. If *cox-1* were similarly up-regulated, siRNA transfection via an

inhaler might be employed to see if similar beneficial results were obtained.

This approach of down-regulating *cox-1* (transiently) could be a good idea to examine first in animal testing and then in clinical trials, as this may result in an increase in apoptosis of cancer cells. However, there are some limitations that cannot be neglected. DNA needs to be introduced specifically to target cells as it would also alter expression in normal cells. In addition, one treatment might not be sufficient so that patients might have to undergo multiple, frequent treatments due to the transient expression. Ultimately, down-regulation of inflammation associated genes using RNAi technology might prove to be life-extending therapy.

## REFERENCES


Abolhoda A, Wilson AE, Ross H, et al (1999). Rapid activation of MDR1 gene expression in human metastatic sarcoma after in vivo exposure to doxorubicin. *Clin Cancer Res*, 5, 3352– 356.

Aliprantis A.O., et al (1999) Cell activation and apoptosis by bacterial lipoproteins through toll-like receptor-2. Science 285:736–739.

Ambudkar SV, Dey S, Hrycyna CA, et al (1999). Biochemical, cellular, and pharmacological aspects of the multi-drug transporter. *Annu Rev Pharmacol Toxicol.* 39:361-398.

Ambudkar SV, Lelong IH, Zhang J, et al (1992). Partial purification and reconstitution of the human multi-drug resistance pump: characterization of the drug-stimulatable ATP hydrolysis. *Proc Natl Acad Sci*, 89, 8472-6.

American Cancer Society. Cancer Facts and Figures (2006). Available at http://www.cancer.org/downloads/STT/CAFF2006PWSecured.pdf. Accessed on August 21, 2009.

American Cancer Society. Cancer Facts and Figures (2007). Available at http://www.cancer.org/downloads/STT/CAFF2007PWSecured.pdf. Accessed on June 21, 2009.

American Cancer Society (2009). Available at http://oralcancerfoundation.org/facts/pdf/Us_Cancer_Facts.pdf. Accessed on June 30, 2009.

American Lung Association (2007). Estimated prevalence and incidence of Lung Disease Report. Available at http://www.lungusa.org/atf/cf/%7B7A8D42C2-FCCA-4604-8ADE-7F5D5E762256%7D/LDD08.PDF. Accessed on August 29, 2009.

American Lung Association (2009). Lung Cancer Fact Sheet. Available at http://www.lungusa.org/lung-disease/lung-cancer/resources/facts-figures/lung-cancer-fact-sheet.html Accessed on January 29, 2010.

Aryal, P (2007). Doxorubicin resistance in a small cell lung cancer cell line can be abolished by siRNA down-regulation of *cox-1*. MS thesis. Ball State University.

Balkwill F, Mantovani A (2001). Inflammation and cancer: back to Virchow? *Lancet* , 357:539-545.

Ballou LR, Botting RM, Goorha S, et al (2000). Nociception in cyclooxygenase isozyme-deficient mice. *Proc. Natl. Acad. Sci. USA* 97:10272–76.

Batist G, Tulpule A, Sinha BK, et al (1986). Overexpression of a novel anionic glutathione transferase in multidrug-resistant human breast cancer cells. *J Biol Chem*, 33, 15544–9.

Borst P, Evers R, Kool M, et al (2000). A family of drug transporters: the multi-drug resistance-associated proteins. *J Natl Cancer Inst*, 92, 1295-302.

Brüne B (2003). "Nitric oxide: NO apoptosis or turning it ON?". *Cell Death Differ.* 10 (8): 864–9.

Centers for Disease Control and Prevention (2007). Preventing and Controlling Cancer: The National Second Leading Cause of Death. May 24. Available at http://cdc.gov/nccdphp/publications/aag/dcpc.htm. Accessed on August 15, 2009.

Chen CJ, Chin JE, Ueda K, et al (1986).Internal duplication and homology with bacterial transport proteins in the mdr1 (Pglycoprotein) gene from multidrug-resistant human cells. *Cell*, 47, 381–9.

Chen G, Goeddel DV (2002). "TNF-R1 signaling: a beautiful pathway". *Science* 296 (5573): 1634–5.

Choi CH (2005). ABC transporters as multi-drug resistance mechanisms and the development of chemosensitizers for their reversal. *Cancer Cell Int*, 5, 30.

Chulada PC, Thompson, MB, Mahler JF, Doyle CM, Gaul BW, Lee C, Tiano HF, Morham SG, Smithies O, and Langenbach R (2000). Genetic disruption of *Ptgs-1*, as well as of *Ptgs-2*, reduces intestinal tumorigenesis in *Min* mice. Cancer Res., *60:* 4705–4708.

Chung SY, Sung MK, Kim NH, et al (2005). Inhibition of Pglycoprotein by natural products in human breast cancer cells. *Arch Pharm Res*, 28, 823-8.

Crofford LJ, Wilder RL, Ristimaki AP, et al (1994). Cyclooxygenase-1 and -2 expression in rheumatoid synovial tissues. Effects of interleukin-1 beta, phorbol ester, and corticosteroids. *J. Clin. Invest.* 93:1095–101

Cole SPC, Bhardwaj G, Gerlach JH, Mackie JE, Grant CE, Almquist KC, Stewart AJ, Kurz EU, Duncan AMV, Deeley RG (1992). Overexpression of a transporter gene in a multidrug-resistant human lung cancer cell line. *Science*. 258: 1650–1654.

Collins LG, Haines C, Perkel R, Enck RE (2007). Lung cancer: diagnosis and management. *Am Fam Physician.*75:56–63.

Conseil G, Baubichon-Cortay H, Dayan G, et al (1998). Flavonoids: a class of modulators with bifunctional interactions at vicinal ATP- and steroid-binding sites on mouse P-glycoprotein. *Proc Natl Acad Sci USA*, 95, 9831-6.

Coussens LM, Werb Z (2002). Inflammation and cancer. *Nature.* 420:860–867.

Daikoku T, Trangush S, Trofimova IN, Dinulescu DM, Jacks T, Nikitin AY, Connolly DC, Sey SK (2006). Cyclooxygenase-1 is overexpressed in multiple genetically engineered mouse models of epithelial ovarian cancer. *Cancer Res* 66: 2527-2531.

Demant EJ, Sehested M, Jensen PB (1990). A model for computer simulation of P-glycoprotein and transmembrane delta pH-mediated anthracycline transport in multi-drug resistant tumor cells. *Biochim Biophys Acta*, 1055, 117–25.

DeWitt DL, Smith WL (1988). Primary structure of prostaglandin G/H synthase from sheep vesicular gland determined from the complementary DNA sequence. *Proc Natl Acad Sci USA*. 85:1412–1416.

Doyle LA, Yang W, Abruzzo LV, et al (1998). A multi-drug resistance transporter from human MCF-7 breast cancer cells. *Proc Natl Acad Sci USA*, 95, 15665-70.

DuBois RN, Abramson SB, Crofford L, Gupta RA, Simon, LS, Van De Putte LB, Lip sky PE (1998). Cyclooxygenase in biology and disease. *FASEB J* 12: 1063–1073.

Dupouy VM, Ferre PJ, Uro-Coste E, and Lefebvre HP (2006). Time course of COX-1 and Cox 2 expression during ischemia-reperfusion in rat skeletal muscle. *Journal of Applied Physiology*. 100: 233-239.

Emedicine (2008). Lung Cancer, Small Cell. Available at http://emedicine.medscape.com/article/358274-media. Accessed on January 30, 2010

Emedicine (2009). Lung Cancer, Small Cell. Available at http://emedicine.medscape.com/article/280104-overview. Accessed on February 10, 2010.

Elmore, S. 2007. Apoptosis: a review of programmed cell death. Toxicol. *Pathol.* 35:495-516.

Fan D, Beltran PJ, O'Brien CA (1994). Reversal of multi-drug resistance. In: Kellen, J.A. (Ed.), Reversal of Multi-drug Resistance in Cancer. CRC Press, Boca Raton, FL, pp. 93– 24.

Fantappie O, Masini E, Sardi I, et al (2002). The MDR phenotype is associated with the expression of COX-2 and iNOS in a human hepatocellular carcinoma cell line. *Hepatology*;35:843–52.

Fardel O, Lecureur V, Guillouzo A (1996). The P-glycoprotein multi-drug transporter. *Gen Pharmacol.*;27:1283-1291.

Fink SL, Cookson BT 2005. Apoptosis, pyroptosis, and necrosis: mechanistic description of dead and dying eukaryotic cells. *Infect. Immun.* 73: 1907–1916.

Fong WF, Wang C, Zhu GY, et al (2007). Reversal of multi-drug resistance in cancer cells by Rhizoma Alismatis extract. *Phytomedicine,* 14, 160–5.

Fornari FA, Randolph JK, Yalowich JC, Ritke MK, Gewirtz DA (April 1994). "Interference by doxorubicin with DNA unwinding in MCF-7 breast tumor cells". *Mol Pharmacol* **45** (4): 649–56.

Gavett SH, Madison SL, Chulada P., Scarborough PE, Qu W, Boyle J.E, Tiano H, Lee CA, Langenbach R, Roggli V, and Zeldin DC (1999). Allergic lung responses are increased in PGH synthase deficient mice. *J. Clin. Invest*. 104: 721-732.

George S, Futscher WB, Isett R, Guzman M, Kunkel M, and Salmon S (2001). cDNA microarray analysis of multi-drug resistance: doxorubicin selection produces multiple defects in apoptosis signaling pathways. *J. Pharmacol. Exp. Therapeutics*. 299: 434-441.

Ghosh J, Myers CE (1997). Arachidonic acid stimulates prostate cancer cell growth: critical role of 5-lipoxygenase. *Biochem. Biophys. Res. Commun.,* 235: 418-423.

Glisson BS (2003) Recurrent small cell lung cancer: update. Semin Oncol 30: 72–78.
Gottesman MM (2002). Mechanisms of cancer drug resistance. *Annu Rev Med*, 53, 615-27.

Gottesman MM, Pastan I (1993). Biochemistry of multi-drug resistance mediated by the multi-drug transporter. *Annu Rev Biochem*, 62, 385–427.

Gottesman MM, Fojo T, Bates SE (2002). Multi-drug resistance in cancer: role of ATP-dependent transporters. *Nat Rev Cancer:* 2:48-58.

Govindan R, Page N, Morgensztern D, et al (2006). Changing epidemiology of small-cell lung cancer in the United States over the last 30 years: analysis of the Surveillance, Epidemiologic, and End Results database. J Clin Oncol ;24:4539-4544.

Grant CE, Valdimarsson G, Hipfner DR, Almquist KC, Cole SPC, Deeley RG (1994) Overexpression of multi-drug resistance-associated protein (MRP) increases resistance to natural product drugs. Cancer Res 54: 357–361.

Grimm D, Kay MA (2007). Therapeutic application of RNAi: Is mRNA targeting finally ready for prime time? *J. Clinical Investigation*: 117: 3633-3641.

Gutman HA (2009). Lung Cancer and Mesothelioma Available at http://www.lungcancerclaims.com/smallcelllungcancer.htm Accessed on August 21, 2009.

Hao XY, Widersten M, Ridderstrom M, et al (1994). Co variation of glutathione transferase expression and cytostatic drug resistance in HeLa cells: establishment of class Mu glutathione transferase M3-3 as the dominating isoenzyme. *Biochem J*, 297, 59–67.

Hawkey CJ (2001). COX-1 and COX-2 Inhibitors. Available at http://www.ncbi.nlm.nih.gov/sites/entrez?cmd=Retrieve&db=PubMed&dopt=AbstractPlus&list_uids=11566042 Accessed on January 2, 2009.

Henshall DC (2007). Apoptosis signaling pathways in seizure-induced neuronal death and epilepsy. *Biochem Soc Trans.* 35(Pt 2):421–423.

Higgins CF (1992). ABC transporters: from microorganisms to man. *Annu Rev Cell Biol*, 8, 67- 113

Hussain SP et al (2007) Inflammation and cancer: an ancient link with novel potentials. *Int. J. Cancer*, 121, 2373–2380

Hwang, D, Scollard D, Byrne J, and Levine E (1998). Expression of cyclooxygenase-1 and cyclooxygenase-2 in human breast cancer. *J. Natl. Cancer Inst*., 90*:* 455–460.

Jain RK (1987). Transport of molecules in the tumor interstitium: a review. *Cancer Res*, 47, 3039–51.

Jemal A, Siegel R, Ward E, et al. Cancer statistics (2006). *CA Cancer J Cli;* 56:106–30

Jemal A, Siegel R, Ward E, et al. Cancer statistics (2008). *CA Cancer J Clin*; 58(2):71-96.

Jemal A, Tiwari RC, Murray T, Ghafoor A, Samuels A, Ward E, Feuer EJ, Thun MJ (2004). Cancer statistics, 2004. *CA Cancer J Clin*; 54: 8-29.

Kang HK, Lee E, Pyo H, Lim SJ (2005). Cyclooxygenase-independent down-regulation of multi-drug resistance-associated protein-1 expression by celecoxib in human lung cancer cells. *Mol Cancer Ther*; 4:1358–1363.

Kellen JA (2003).The reversal of multi-drug resistance: an update. *J Exp Ther Oncol*, 3,5-13

Kerr JF, Wyllie AH, Currie AR (August 1972). "Apoptosis: a basic biological phenomenon with wide-ranging implications in tissue kinetics". *Br. J. Cancer* 26 (4): 239–57. PMID 4561027.

Krishna R, Mayer LD (2000). Multi-drug resistance (MDR) in cancer. Mechanisms, reversal using modulators of MDR and the role of MDR modulators in influencing the pharmacokinetics of anticancer drugs. *Eur J Pharm Sci.*;11:265-283.

Kuper H, Adami HO, Trichopoulos D. Infections as a major preventable cause of human cancer. *J Intern Med.* 2000;248:171–183.

Lampiasi N, Fodera D, D'Alessandro N, Cusimano A, Azzolina A, Tripodo C, Florena AM, Minervini MI, Notarbartolo M, Montalto G, Cervello M. The selective cyclooxygenase-1 inhibitor SC-560 suppresses cell proliferation and induces apoptosis in human hepatocellular carcinoma cells. *Int J Mol Med* 2006; 17: 245-252

Langenbach R, Morham SG, Tiano HF et al (1995) Prostaglandin synthase 1 gene disruption in mice reduces arachidonic acid-induced inflammation and indomethacin induced gastric ulceration. Cell 83:483–492

Lazebnik, Y.A., Kaufmann, S.H., Desnoyers, S., Poirier, G.G., Earnshaw, W.C (1994). Cleavage of poly(ADP-ribose) polymerase by a proteinase with properties like ICE. *Nature* 371:346-347

Leonard GD, Fojo T, Bates SE (2003). The role of ABC transporters in clinical practice. *Oncologist*, 8, 411–24.

Limtrakul P, Siwanon S, Yodkeeree S, et al (2007). Effect of Stemona curtisii root extract on P-glycoprotein and MRP-1 function in multidrug-resistant cancer cells. *Phytomedicine*, 14, 381–9.

Ling Li, Qiangrong Pan, Meng Sun, et al (2007). Dibenzocyclooctadiene lignans — A class of novel inhibitors of multi-drug resistance-associated protein. *Life Sciences*, 80, 741–8.

Li W, et al (2008). Effects of a cyclooxygenase-1- selective inhibitor in a mouse model of ovarian cancer, administered alone or in combination with ibuprofen, a nonselective cyclooxygenase inhibitor. *Medical Oncology*.

Loo TW, Clarke DM (2001). Defining the drug-binding site in the human multi-drug resistance P-glycoprotein using a methanethiosulfonate analog of verapamil, MTS-verapamil. *J Biol Chem*, 276, 14972-9.

Lowe SW, Lin AW (2000). Apoptosis in cancer. *Carcinogenesis*.;21:485–495.

Martin SJ, Reutelingsperger CP, McGahon AJ, et al (1995). Early redistribution of plasma membrane phosphatidylserine is a general feature of apoptosis regardless of the initiating stimulus: inhibition by overexpression of Bcl-2 and Abl. *J Exp Med.*;182(5):1545-1556.

Mayne ST et al (1999) Previous lung disease and risk of lung cancer among men and women nonsmokers. *Am. J. Epidemiol.*, 149, 13–20.

McAdam BF, Mardini IA, Habib A, et al (2000). Effect of regulated expression of human cyclooxygenase isoforms on eicosanoid and isoeicosanoid production in inflammation. *J. Clin. Invest.*105:1473–82

Meijer C, Mulder NH, Hospers GA, Uges DR, de Vries EG. The role of glutathione in resistance to cisplatin in a human small cell lung cancer cell line. BrJ Cancer 1990;62:72-7.

Merlie JP, Fagan D, Mudd J, Needleman P (1988). Isolation and characterization of the complementary DNA for sheep seminal vesicle prostaglandin endoperoxide synthase (cyclooxygenase). *J Biol Chem*.;263:3550–3553.

Momparler RL, Karon M, Siegel SE, Avila F (August 1976). "Effect of adriamycin on DNA, RNA, and protein synthesis in cell-free systems and intact cells". *Cancer Res* **36** (8): 2891–5.

Moller HJ, Heinegard D, Poulsen JH. Combined alcian blue and silver staining of subnanogram quantities of proteoglycans and glycosaminoglycans in sodium dodecylsulfate-polyacrylamide gels. *Anal Biochem*. 1993;15;209(1):169-75.

Morham SG, Langenbach R, Loftin CD et al (1995) Prostaglandin synthase 2 gene disruption causes severe renal pathology in the mouse. *Cell* 83:473–482

Morita, I., Schindler, M., Regier, M. K., Otto, J. C., Hori, T., DeWitt, D. L., and Smith, W. L. (1995) Different intracellular locations for prostaglandin endoperoxide H synthase-1 and -2. *J. Biol. Chem.* 270, 10902–10908.

Müller M, Meijer C, Zaman GJ, Borst P, Scheper RJ, Mulder NH, de Vries EG, Jansen PL (1994) Overexpression of the gene encoding the multidrug resistance-associated protein results in increased ATP-dependent glutathione *S*-conjugate transport. *Proc Natl Acad Sci USA* **91**: 13033–13037

Munger K, Howley PM. Human papillomavirus immortalization and transformation functions. *Virus Res.* 2002;89:213–228.

Murphy KM, Ranganathan V, Farnsworth ML, Kavallaris M, Lock RB (2000). "Bcl-2 inhibits Bax translocation from cytosol to mitochondria during drug-induced apoptosis of human tumor cells". *Cell Death Differ.* 7 (1): 102–11.

Nakamura M, Abe Y, Katoh Y et al (2000). A case of pulmonary adencarcinoma with overexpression of multi-drug resistance associated protein and p53 aberration. *Anticancer Res*, 20, 1921–5.

Narko, K., Ristimaki, A., MacPhee, M., Smith, E., Haudenschild, C. C., and Hla, T (1997). Tumorigenic transformation of immortalized ECV endothelial cells by cyclooxygenase- 1 overexpression. J. Biol. Chem., *272:* 21455–21460.

National Cancer Institute (2007). Cancer trends progress report. Available at http://progressreport.cancer.gov/doc_detail.asp?pid=1&did=2007&chid=75&coid=726&mid. Accessed on August 21, 2009.

National Cancer Institute, Bethesda, MD (2004). The Seer Cancer Statistics review. http://www.cancer.gov/newscenter/pressreleases/ProgressReport2007.

National Cancer Institute (2009). Inflammation and Cancer. Available at http://dcb.nci.nih.gov/thinktank/Executive_Summary_of_Inflammation_and_Cancer_ThinkTank.cfm
Accessed on August 30, 2009

Nugent JL, Bunn PA Jr, Matthews MJ, et al (1979). CNS metastases in small cell bronchogenic carcinoma: increasing frequency and changing pattern with lengthening survival. *Cancer*; 44:1885-1893.

Olsen JH, Friis S, Poulsen AH, Fryzek J, Harving H, Tjonneland A, Sorensen HT, Blot W (2008). Use of NSAIDs, smoking and lung cancer risk. *Br J Cancer*; 98:232–7.

Oncology Channel (1999). Lung cancer treatment. Available at http://www.oncologychannel.com/lungcancer/treatment.shtml . Accessed on August 21, 2009

Osset M, Pinol M, Fallon MJM, de Llorens R, Cuchillo CM. Interference of the carbohydrate moiety in Coomassie Brilliant Blue R-250 protein staining. *Electrophoresis*. 1989;10(4):271-3.

Patel VA, Dunn MJ, Sorokin A (2002). Regulation of MDR-1 (P-glycoprotein) by cyclooxygenase-2. J Biol Chem;277:38915–20.

Pepin P, Bouchard L, Nicole P, Castonguay A (1992). Effects of sulindac and oltipraz on the tumorigenicity of 4-(methylnitrosamino)1-(3-pyridyl)-1-butanone in A/J mouse lung. *Carcinogenesis*. 13:341–8.

Popov SG, Villasmil R, Bernardi J (April 2002). "Lethal toxin of Bacillus anthracis causes apoptosis of macrophages". *Biochem. Biophys. Res. Commun.*293 (1): 349–55.

Ratnasinghe D, Daschner PJ, Anver MR, et al (2001). Cyclooxygenase-2, P-glycoprotein-170 and drug resistance; is chemoprevention against multi-drug resistance possible? *Anticancer Res*; 21:2141–7.

Reich A, Spering C, Schulz JB (2008) Death receptor Fas (CD95) signaling in the central nervous system: tuning neuroplasticity? *Trends Neurosci* 31:478–486.

Riccardi, C., and I. Nicoletti. 2006. Analysis of apoptosis by propidium iodide staining and flow cytometry. Nat. Protoc. 1:1458-1461.

Riely GJ, Kris MG, Rosenbaum D, Marks J, Li A, Chitale DA, Nafa K, Riedel ER, Hsu M, Pao W, *et al.* Frequency and distinctive spectrum of KRAS mutations in never smokers with lung adenocarcinoma. *Clin Cancer Res* 2008;14:5731–5734.

Riordan JR, Deuchars K, Kartner N, et al (1985). Amplification of P-glycoprotein genes in multidrug-resistant mammalian cell lines. *Nature*, 316, 817-9.

Rossi SE, Erasmus JJ, McAdams HP, Sporn TA, Goodman PC (2000). Pulmonary drug toxicity: radiologic and pathologic manifestations. Radiographics; 20:1245–1259.

Saijo N (2003). Progress in treatment of small-cell lung cancer: role of CPT-11. *Br J Cancer*; 89: 2178-83.

Schoenlein PV (1994). Role of gene amplification in drug resistance. In: Goldstein, L.J., Ozols, R.F. (Eds.), Anticancer Drug Resistance: Advances in Molecular and Clinical Research. Kluwer, Boston, MA, pp. 167–200.

Schonbeck U, Sukhova GK, Graber P, et al (1999). Augmented expression of cyclooxygenase-2 in human atherosclerotic lesions. *Am. J. Pathol.* 155:1281–91.

Schreiber D, Rineer J, Vongtama D, et al (2008). Surgery for limited-stage small cell lung cancer,should the paradigm shift?A SEER-based analysis. *J Clin Oncol (Supplement)* ;26:403s.

Schreinemachers, D.M., and Everson, R.B (1994). Aspirin use and lung, colon, and breast cancer incidence in a prospective study. *Epidemiology*. 5: 138-146.

Schroeijers AB, et al (2001). Detection of the $M_r$ 110,000 lung resistance-related protein LRP/MVP with monoclonal antibodies. *The Journal of Histochemistry and Cytochemistry* 49: 1379-1385.

Schroeijers AB, et al (2000). The Mr 193,000 vault protein is up-regulated in multidrug-resistant cancer cell lines. *Cancer Research* 60, 1104-1110.

Seute T, Leffers P, ten Velde GPM, Twijnstra A (2004). Neurologic disorders in 432 consecutive patients with small cell lung carcinoma. *Cancer*; 100:801-806.

Shuzhong Z, Xinning Y, Robert AC, et al (2005). Structure activity relationships and quantitative structure activity relationships for the flavonoid-mediated inhibition of breast cancer resistance protein. *Biochem Pharmacol*, 70, 627–39.

Siva AC, Raval-Fernandes S, Stephen AG, La Femina MJ, Scheper RJ, Kickhoefer VA, and Rome LH (2001). Up-regulation of vaults may be necessary but not sufficient for multi-drug resistance. *Int J Cancer*: 92:195-202.

Smith JB, Willis AL (1971). Aspirin selectively inhibits prostaglandin production in human platelets. *Nat. New Biol.*;231:235–237

Smith WL, DeWitt DL (1996) in *Advances in Immunology* (Dixon, F. J., ed) Vol. 62, pp. 167–215, Academic Press, Orlando, FL.

Smith WL, DeWitt DL, Garavito RM (2000): Cyclooxygenases: Structural, cellular, and molecular biology. *Annu Rev Biochem.* 69: 145–182.

Smith WL, Langenbach R (2001). Why there are two cyclooxygenase isozymes. *J. Clin. Invest.* 107:1491–95

Sorokin A. Cyclooxygenase-2: potential role in regulation of drug efflux and multi-drug resistance phenotype. *Curr Pharm Des* 2004;10:647–57.

Statistics and Information Department, Minister's Secretariat (2002) Ministry of Health, Labour, and Welfare Vital Statistics of Japan (Ministry of Health, Labour, and Welfare, Tokyo).

Susin SA, Lorenzo HK, Zamzami N (1999). "Molecular characterization of mitochondrial apoptosis-inducing factor". *Nature*397 (6718): 441–6.

Tsujii M, Kawano S, Tsuji S, Sawaoka H, Hori M, and DuBois RN (1998). Cyclooxygenase regulates angiogenesis induced by colon cancer cells. Cell, *93:*705–716.

U.S. National Institutes of Health. National Cancer Institute (2007). A Snapshot of Lung Cancer. December. Available at http://planning.cancer.gov/disease/Lung-Snapshot.pdf. Accessed on September 10, 2009.

U.S. National Institutes of Health. National Cancer Institute (2008). A Snapshot of Lung Cancer. December. Available at http://planning.cancer.gov/disease/Lung-Snapshot.pdf. Accessed on September 10, 2009.

Vakkila J, Lotze M. Inflammation and necrosis promote tumor growth. *Nat Rev Immunol* 4: 641–648, 2004.

Vane JR, YS Bakhle, RM Botting (1998). Cyclooxygenases 1 and 2. *Annu. Rev. Pharmacol. Toxicol.* 38:97-120.

Vane JR (1971). Inhibition of prostaglandin synthesis as a mechanism of action for the aspirin-like drugs. *Nature New Biology 231:232–235.*

Vardeh D, Wang D, Costigan M, et al (2009). COX2 in CNS neural cells mediates mechanical inflammatory pain hypersensitivity in mice. *J. Clin. Invest.* 119:287–94.

Wajant H (2002). "The Fas signaling pathway: more than a paradigm". *Science* 296 (5573): 1635–6.

Wang X., Christiani D. C., Wiencke J. K., Fischbein M., Xu X., Cheng T. J., Mark E., Wain J. C., Kelsey K. T. Mutations in the p53 gene in lung cancer are associated with cigarette smoking and asbestos exposure. Cancer Epidemiol. Biomark. Prev., 4: 543-548, 1995.

Wang X et al (2001;) The expanding role of mitochondria in apoptosis. Genes Dev 15:2922–2933.

Wisconsin Veterinary Diagnostic Laboratory (2009). Available at http://www.wvdl.wisc.edu/PDF/WVDL.Info.PCR_Ct_Values.pdf. Accessed on June 27, 2010.

Wu AH et al (1995) Previous lung disease and risk of lung cancer among lifetime nonsmoking women in the United States. Am. J. Epidemiol., 141, 1023–1032.

Wu KK (1996) Cyclooxygenase 2 induction: molecular mechanism and pathophysiologic roles. *J. Lab. Clin. Med.*, 128, 242–245.

Xu D, Lu Q, Hu X (2006). Down-regulation of P-glycoprotein expression in MDR breast cancer cell MCF-7/ADR by honokiol. *Cancer Letters*. 243, 274–80.

Yokoyama C, Takai T, Tanabe T (1988). Primary structure of sheep prostaglandin endoperoxide synthase deduced from cDNA sequence. *FEBS Lett*. 231:347–351.

Young LC, Campling BG, Cole SP, Deeley RG, Gerlach JH (2001). Multi-drug resistance proteins MRP3, MRP1, and MRP2 in lung cancer: correlation of protein levels with drug response and messenger RNA levels. *Clin Cancer Res*; 7:1798–804.

Yu Y, Cheng Y, Fan J, et al (2005). Differential impact of prostaglandin H synthase 1 knockdown on platelets and parturition. *J. Clin. Invest.* 115:986–95.

Zaman GJR, Flens MJ, Van Leusden MR, de Haas M, Mulder HS, Lankelma J, Pinedo HM, Scheper RJ, Baas F, Broxterman HJ, Borst P (1994) The human multi-drug resistance-associated protein MRP is a plasma membrane drug-efflux pump. *Proc Natl Acad Sci* USA 91: 8822–8826.

Zhang B, Wang Q, Pan X (2007). MicroRNAs and their regulatory roles in animals and plants. *J Cell Physiol.* 210(2):279-89

Zijlstra, J. G., de Vries, E. G. E., Mulder, N. H., de Ley, L., and de Jong, B. Adriamycin (ADR) resistance in a human small cell lung cancer (SCLC) cell line. Proc. Am. Assoc. Cancer Res., 27:1083, 1986.